DOE/ET/20041--T2

KINETIC INVESTIGATION OF WOOD PYROLYSIS

by

Franz Thurner
Uzi Mann
Steven R. Beck

Department of Chemical Engineering
Texas Tech University
Lubbock, Texas 79409

MASTER

June 1980

Prepared for the

U.S. Department of Energy
Division of Solar Energy
Fuels From Biomass Systems Branch

Contract No. DE-AC04-79ET20041

DISCLAIMER

THIS PAGE

WAS INTENTIONALLY

LEFT BLANK

ABSTRACT

The objective of this investigation was to determine the kinetics of the primary reactions of wood pyrolysis. A new experimental method was developed which enabled us to measure the rate of gas, tar, and char production while taking into account the temperature variations during the wood heating up.

The experimental method developed did not require any sophisticated instruments. It facilitated the collection of gas, tar and residue (unreacted wood and char) as well as accurate measurement of the temperature inside the wood sample. Expressions relating the kinetic parameters to the measured variables were derived.

The pyrolysis kinetics was investigated in the range of 300 to 400°C at atmospheric pressure and under nitrogen atmosphere. Reaction temperature and mass fractions of gas, tar, and residue were measured as a function of time. Assuming first-order reactions, the kinetic parameters were determined using differential method. The measured activation energies of wood pyrolysis to gas, tar, and char were 88.6, 112.7, and 106.5 kJ/mole, respectively. These kinetic data were then used to predict the yield of the various pyrolysis products. It was found that the best prediction was obtained when an integral-mean temperature obtained from the temperature-time curve was used as reaction temperature.

The pyrolysis products were analyzed to investigate the influence of the pyrolysis conditions on the composition. The gas consisted mainly of carbon dioxide, carbon monoxide, oxygen, and C_3^+-compounds. The gas composition depended on reaction time as well as reactor temperature. The tar analysis indicated that the tar consisted of about seven compounds. Its major compound was believed to be levoglucosan. Elemental analysis for the char showed that the carbon content increased with increasing temperature.

TABLE OF CONTENTS

LIST OF TABLES

THIS PAGE

WAS INTENTIONALLY

LEFT BLANK

1. INTRODUCTION

The chemical industry has grown rapidly during the past fifty years in both volume and sophistication of products. Stimulated by abundant and inexpensive supplies of crude oil as a raw material, synthetic organic materials have entered and enriched every facet of our society. Our standard of living is inextricably bound to synthetic organic materials.

As a consequence of the recent substantial increase in the price of crude oil, as well as the concern about its availability, attention has been focused on alternative feedstocks. Considerable effort is being expended in converting coal into raw materials for chemical processes. Attention is also being given to converting biomass, a renewable resource, to chemical feedstocks.

Wood is probably the most important renewable biomass (1). In order to use wood as a source of hydrocarbon feedstocks it must be converted first into compounds of simple structure. One of the most important ways to do so is wood pyrolysis. Wood pyrolysis is the thermal decomposition of wood at high temperatures in the absence of oxygen. Especially, high temperature pyrolysis favors the formation of low molecular hydrocarbons like methane, ethylene, and acetylene (2).

Wood pyrolysis has a long history, dating back to ancient Chinese and Egyptians, who used the tarry products for embalming (3). In the early 1900's and later briefly during World War II wood pyrolysis was used to obtain a variety of products including charcoal, acetic acid, wood alcohol, tar, and gases. After World War II pyrolysis processes were abandoned in favor of the more economical processes developed by the petrochemical industry based on efficient thermal and catalytic cracking of crude oil.

Nowadays the conversion of biomass or cellulosic municipal waste into more valuable products by means of pyrolysis becomes again economically feasible. The implementation of such processes depends to a large extent on reliable design of large-scale units, in which the pyrolysis reactor plays an important role. Proper design of such a reactor requires understanding of the mechanism and knowledge of the kinetics of wood pyrolysis. Many investigators have reported data on wood pyrolysis and other related substances in terms of weight loss as a function of time. However, such data are not suitable to predict the yield of the various pyrolysis products. The objective of the present investigation was, therefore, to determine the kinetics of the different simultaneous reactions taking place during wood pyrolysis.

Before reviewing the literature on wood pyrolysis it is worthwhile to recapitulate the composition of wood. Wood, on a dry basis, consists mainly of three components: cellulose, hemicellulose and lignin. These components are composed of large molecules and constitute from 95 to 98 percent of the wood. The remaining 2 to 5 percent are lower molecular weight compounds, called extractives. The amount of each component, especially the hemicellulose, lignin and extractives varies between hardwoods and softwoods (see Table 1). Freshly cut wood usually contains 50 percent or more moisture.

Noting that wood consists mainly of cellulose, hemicellulose and lignin, Brown (5) found out experimentally that the product yield obtained when wood is completely pyrolyzed is about the same as the yield obtained by separately pyrolyzing proportional amounts of these wood constituents. When wood is heated in the absence of oxygen, the hemicellulose decomposes first, mainly

Table 1: Chemical Composition of Dry Wood (4). (Weight Percent)

	Softwoods	Hardwoods
Cellulose	42 ± 2	45 ± 2
Hemicellulose	27 ± 2	30 ± 5
Lignin	28 ± 3	20 ± 4
Extractives	3 ± 2	5 ± 3

between 200 and 260°C, followed by the cellulose at 240 to 350°C. The lignin is gradually decomposed between 280 and 500°C. The products of wood pyrolysis can be divided into three fractions (3):

- a carbonaceous solid (char),
- a mixture of liquid compounds (tar), and
- a mixture of gases.

Cellulose and hemicellulose decompose mostly to volatile products, while lignin is pyrolyzed predominantly to char (5).

The amount and distribution of the pyrolysis products depend on heating rate, temperature, and pressure. The presence of inorganic compounds such as zinc chloride has catalytic effects. At slow heating rate more char, less tar, and some gas are formed. On the other hand, at rapid heating rate less char and more tar and gases are generated. The final temperature achieved affects the yield of tar. At higher temperature the tar is decomposed to char and gases (4). High pressure favors the formation of char over gas (7). Heating wood in the presence of acidic or basic catalysts, such as phosphoric acid, diammonium phosphate, diphenyl phosphate and zinc chloride, increases charring with a proportionate decrease in tar formation (3, 16).

Due to the wide variety of products obtained from wood pyrolysis, the kinetics is quite complex. Shafizadeh (3) lumped together different compounds and proposed a simplified mechanism shown in Figure 1. This mechanism consists of three primary and two secondary reactions. The primary reactions (reaction 1, 2, and 3) are the decomposition of wood, whereas the secondary reactions (reaction 4, 5) are the decomposition of the tar. Reaction 1 is believed to consist of reactions such as depolymerization, hydrolysis, oxidation, dehydration, and decarboxylation. These reactions commence with considerable rate at about 250°C. Reaction 2 is the formation of tar and takes place above 250°C. Reaction 3 represents fragmentation of wood.

Kinetic data of the primary and secondary reactions in Figure 1 have not been found in the literature. This is probably due to the limitations of the experimental methods used to determine kinetic parameters of wood pyrolysis. The most commonly-used method is the measurement of a wood sample weight loss as a function of time or temperature, called thermogravimetric analysis (TGA). There are two different types of thermogravimetric analyses: static or isothermal TGA monitoring the weight loss as a function of time at a fixed temperature and dynamic or non-isothermal TGA monitoring the weight loss as a function of temperature at a fixed heating rate. Both methods suffer from two major drawbacks when using them for determination of kinetics: First, the commercially available instruments allow one to measure only the sample weight loss as a function of time or temperature. Therefore, the kinetic data obtained by TGA account only for the reactions to volatile products (reaction 1 + 2). Second, in most cases the temperature variation during the heating-up period is neglected and the inert gas temperature is usually

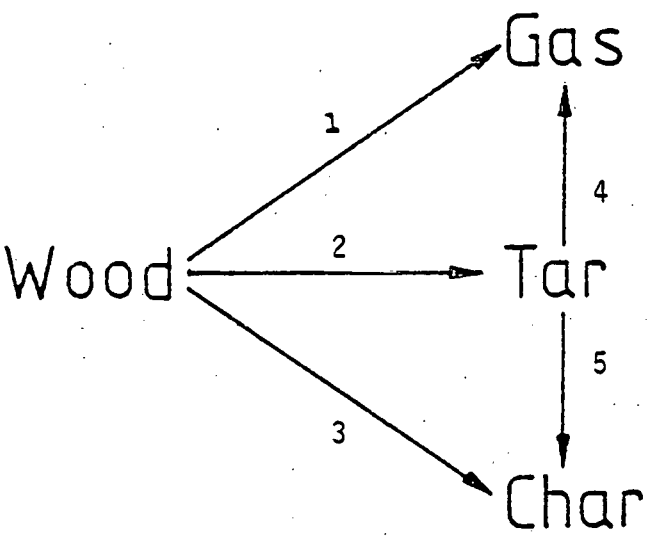

Figure 1: Suggested Mechanism for Wood Pyrolysis (3)

used as the reaction temperature. This temperature is not always the same as the actual reaction temperature inside the sample. This inaccurate temperature measurement is probably the main reason for the wide variations of the activation energy E for the weight loss reaction reported in the literature (8, 12, 13, 14, 15). Antal et al. (8) compared the kinetic data reported by different investigators. Most of them assumed a first order kinetics. Antal indicated that researchers who measured the reaction temperature accurately obtained activation energies E in the range of 109 to 139 kJ/mole.

Another experimental method used to investigate the wood thermal behavior is differential thermal analysis (DTA). This method is mainly used to estimate the heat of reaction. However, no kinetic data obtained from DTA have been reported in the literature reviewed. In DTA, the temperature difference between a thermocouple embedded inside the sample and another thermocouple placed in an inert material is measured. If the reaction is endothermic the sample temperature lags behind the reference temperature, whereas for an exothermic reaction the sample temperature leads the reference temperature. This method gives a measure of the energy absorbed or released during pyrolysis. Pyrolysis of cellulosic material is an endothermic reaction and the reported heat of pyrolysis is about 268 J/g (7).

2. THEORETICAL CONSIDERATIONS

As suggested by Shafizadeh (3), wood is pyrolyzed into gas, char and tar according to three parallel reactions (reaction 1, 2, 3), referred to as primary reactions. The tar decomposes into gas and char according to two parallel reactions (reaction 4, 5), referred to as secondary reactions.

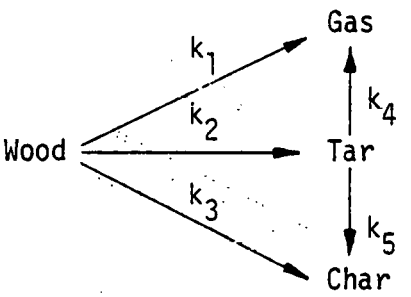

(2-1)

Each product in (2-1) represents a sum of numerous components which are lumped together to simplify the analysis. The composition of each product depends, among other things, on the conditions under which the products are collected.

The reaction rate constants of all of these five reactions can be determined by measuring the amount of each species in (2-1) as a function of time. The reaction rate constants of the primary reactions can be determined more conveniently by removing the tar from the reaction zone and thus avoiding the secondary reactions.

Assuming that each primary reaction is first-order, the formation or disappearance rate of each component is given by

$$\frac{dm_W(t)}{dt} = -(k_1 + k_2 + k_3)m_W(t) \qquad (2\text{-}2)$$

$$\frac{dm_G(t)}{dt} = k_1\, m_W(t) \qquad (2\text{-}3)$$

$$\frac{dm_T(t)}{dt} = k_2\, m_W(t) \tag{2-4}$$

$$\frac{dm_C(t)}{dt} = k_3\, m_W(t) \tag{2-5}$$

These relations are expressed in terms of mass rather than mole. It is more convenient to write these equations in terms of mass fraction by dividing them by the initial mass of the wood $m_W(0)$, i.e.

$$\frac{dw_W(t)}{dt} = -(k_1 + k_2 + k_3)w_W(t) \tag{2-6}$$

$$\frac{dw_G(t)}{dt} = k_1\, w_W(t) \tag{2-7}$$

$$\frac{dw_T(t)}{dt} = k_2\, w_W(t) \tag{2-8}$$

$$\frac{dw_C(t)}{dt} = k_3\, w_W(t) \tag{2-9}$$

For isothermal pyrolysis (2-6) to (2-9) can be solved analytically. The solutions subject to the initial conditions $w_W = 1$ and $w_G = w_T = w_C = 0$ at $t = 0$ are

$$w_W(t) = \exp(-kt) \tag{2-10}$$

$$w_G(t) = \frac{k_1}{k}[1 - \exp(-kt)] \tag{2-11}$$

$$w_T(t) = \frac{k_2}{k}[1 - \exp(-kt)] \tag{2-12}$$

$$w_C(t) = \frac{k_3}{k}\,[1 - \exp(-kt)] \tag{2-13}$$

where $k = k_1 + k_2 + k_3$ is the overall rate constant of wood pyrolysis.

Primarily, wood is decomposed by three independent reactions (reaction 1, 2, 3). To determine their rate constants it is, therefore, necessary to measure the mass fraction of any three components as a function of time. Experimentally, the mass fraction of gas and tar can be measured directly. But it is impossible to measure the mass fraction of either unreacted wood or char separately, because both are collected together as solid residue. Therefore, another way must be developed to determine the reaction rate constants.

Using the overall mass balance, the mass fraction of the residue is related to the mass fractions of gas and tar by

$$w_R(t) = w_W(t) + w_C(t) = 1 - w_G(t) - w_T(t) \tag{2-14}$$

At isothermal conditions, a relation between the char mass fraction and the residue mass fraction can be obtained by combining (2-11), (2-12) and (2-13) with (2-14).

$$\frac{w_C(t)}{w_G(t) + w_T(t)} = \frac{w_C(t)}{1 - w_R(t)} = \frac{k_3}{k_1 + k_2} \tag{2-15}$$

Note that (2-15) is independent of the time and also valid for long reaction time or high conversion. For complete conversion $w_W(t \to \infty) = 0$, and from (2-14) $w_R(t \to \infty) = w_C(t \to \infty)$. Thus, (2-15) can be expressed in terms of $w_R(t \to \infty)$

$$\frac{w_R(t \to \infty)}{1 - w_R(t \to \infty)} = \frac{k_3}{k_1 + k_2} \tag{2-16}$$

This relation indicates that $k_3/(k_1 + k_2)$ can be easily determined by measuring the residue mass fraction at complete conversion. Thus the mass fraction of char at any time can be calculated by combining (2-15) and (2-16)

$$w_C(t) = \frac{w_R(t \to \infty)}{1 - w_R(t \to \infty)} [w_G(t) + w_T(t)] \qquad (2\text{-}17)$$

The wood mass fraction, $w_W(t)$, can be derived by using the overall mass balance, $w_W(t) = 1 - w_G(t) - w_C(t) - w_T(t)$, and (2-17), i.e.,

$$w_W(t) = \frac{w_R(t) - w_R(t \to \infty)}{1 - w_R(t \to \infty)} = 1 - \frac{\Delta w_R(t)}{1 - w_R(t \to \infty)} \qquad (2\text{-}18)$$

where $\Delta w_R(t) = 1 - w_R(t)$.

Equations (2-15) to (2-18) are valid only for isothermal pyrolysis. However, isothermal conditions are rarely achieved experimentally due to the heating-up of the sample. In principle, for nonisothermal pyrolysis the kinetic parameters can be estimated by first integrating (2-6) to (2-9) according to the temperature variations with time and nonlinear parameter optimization. This is a difficult and cumbersome procedure. However, in many cases $k_3/(k_1 + k_2)$ varies very little over a wide temperature range. This occurs when the activation energy of the char formation reaction (reaction 3) is about the same as the activation energy for the weight loss reaction (reaction 1 + 2). This assumption can be readily verified experimentally by determining whether $w_R(t \to \infty)$ is constant at different reaction temperatures.

When this assumption is valid, the reaction rate constant of reaction 3 can be calculated by using (2-16)

$$k_3 = \frac{w_R(t \to \infty)}{1 - w_R(t \to \infty)} [k_1 + k_2] \tag{2-19}$$

The reaction rate constants of reaction 1 and 2 can be determined from the experimental composition-time curves for gas and tar by the differential method, i.e.,

$$k_1 = \frac{1}{w_W(t)} [\frac{dw_G(t)}{dt}] \tag{2-20}$$

$$k_2 = \frac{1}{w_W(t)} [\frac{dw_T(t)}{dt}] \tag{2-21}$$

The mass fraction of unreacted wood, $w_W(t)$, is calculated by (2-18). Figure 2 illustrates the determination of these parameters from experimental data.

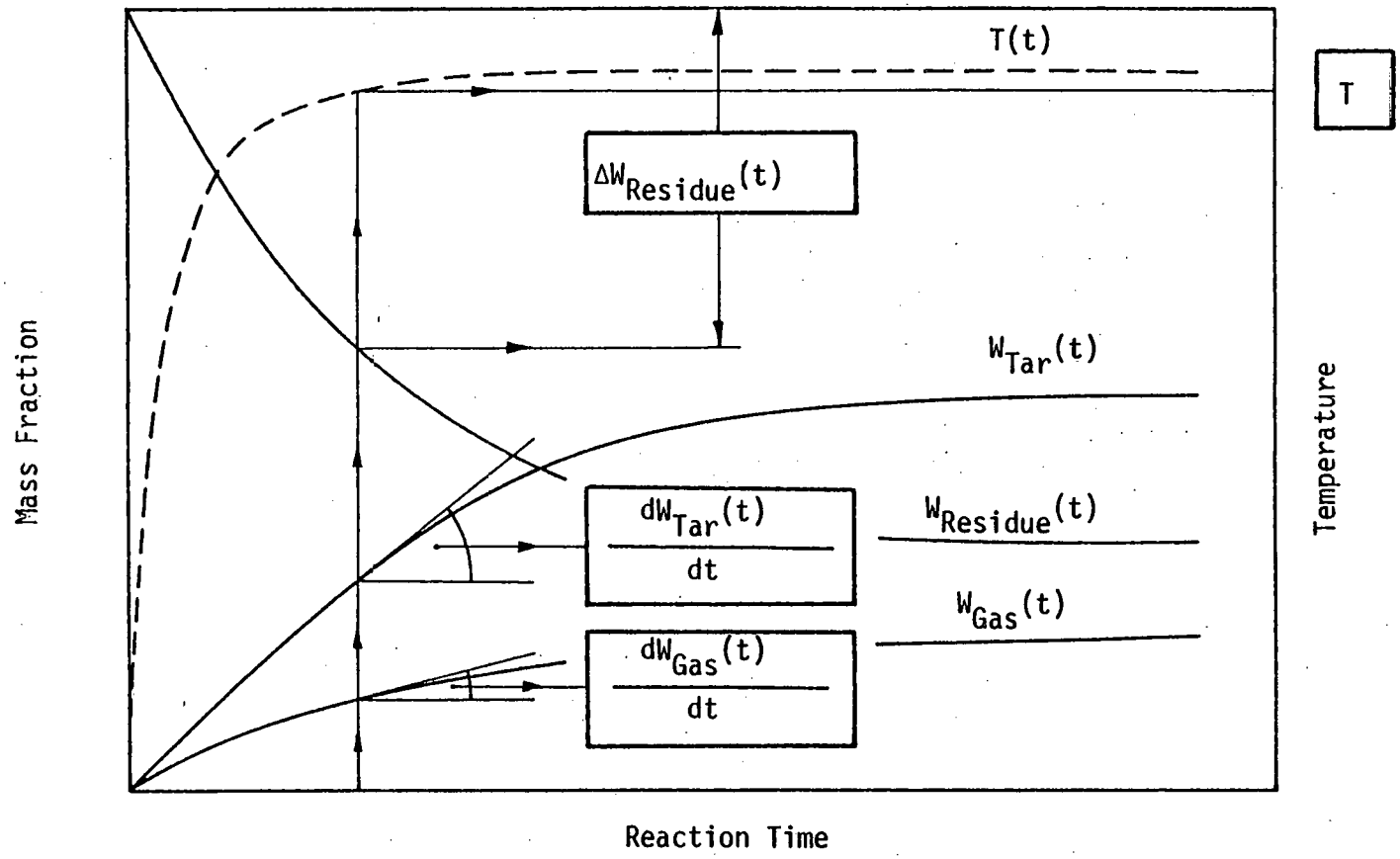

Figure 2: Determination of the Kinetics from Experimental Data

3. EQUIPMENT AND PROCEDURE

The experimental system used in this investigation was designed to pyrolyze wood and to measure the mass of residue, tar, and gas as a function of time at different reactor temperatures. The objective was to construct a simple and inexpensive system which provides accurate data without the need of sophisticated instruments.

3.1 Description of the Equipment

A flow diagram of the experimental system is shown in Figure 3. The system can be divided into three sections:

- reactor section,
- gas supply section, and
- gas collection section.

The reactor was the heart of the system. Details and dimensions of the reactor are given in Figure 4 and a photograph of the reactor is shown in Figure 5. The reactor consisted of three parts:

- reaction chamber,
- cooler, and
- condenser.

The wood pyrolysis took place in the reaction chamber which was heated by a heater to maintain the desired temperature. The chamber was made of a 1 inch (25 mm), schedule 40, stainless steel tube, 13 inches (330 mm) long. This tube was heated by two Lindberg semi-cylindrical electrical resistance heating units mounted arount it. Both heating units were rated to 435 watts/115 volts when connected together. The heater was

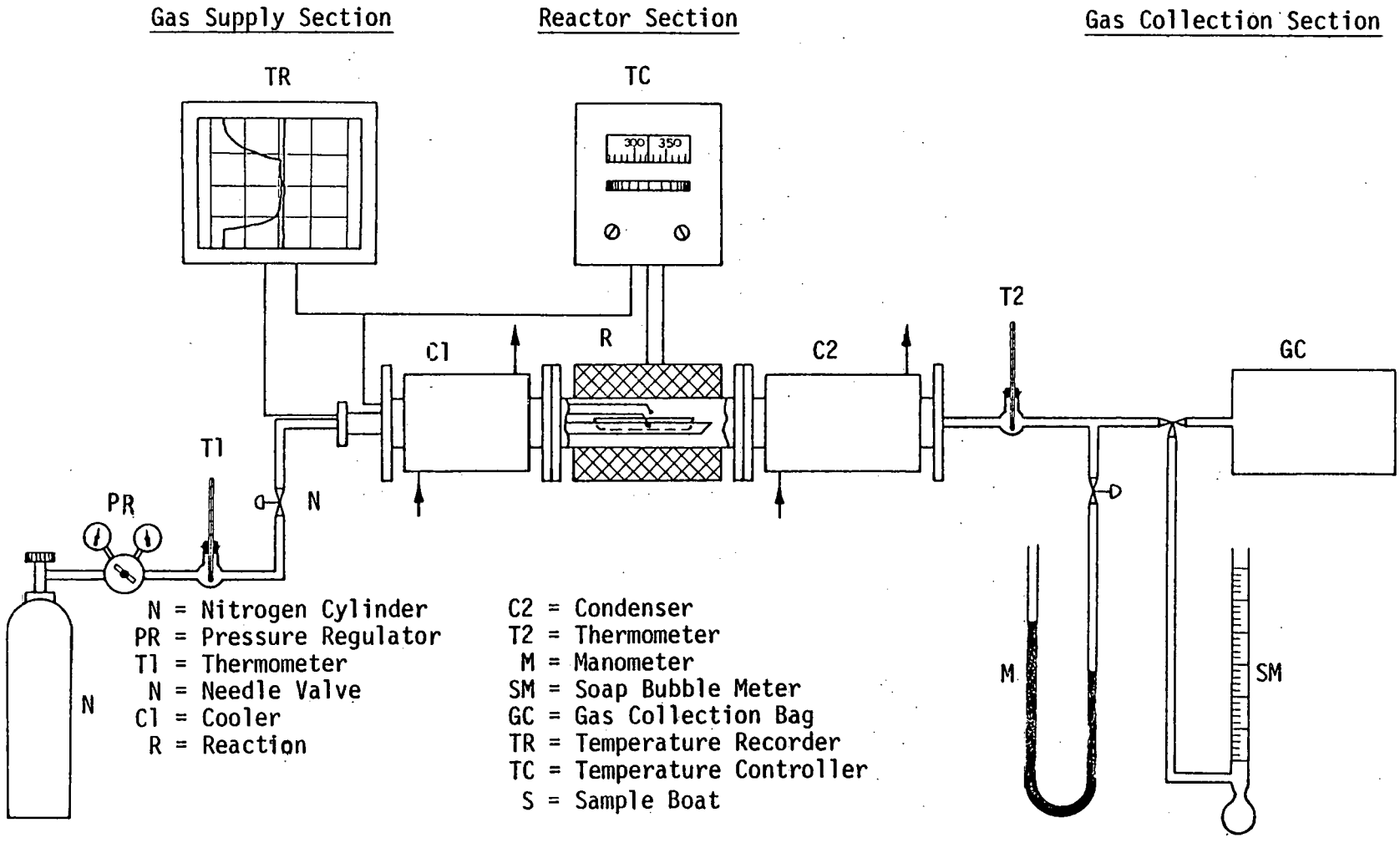

Figure 3: Bench Scale Reactor - Flow Diagram

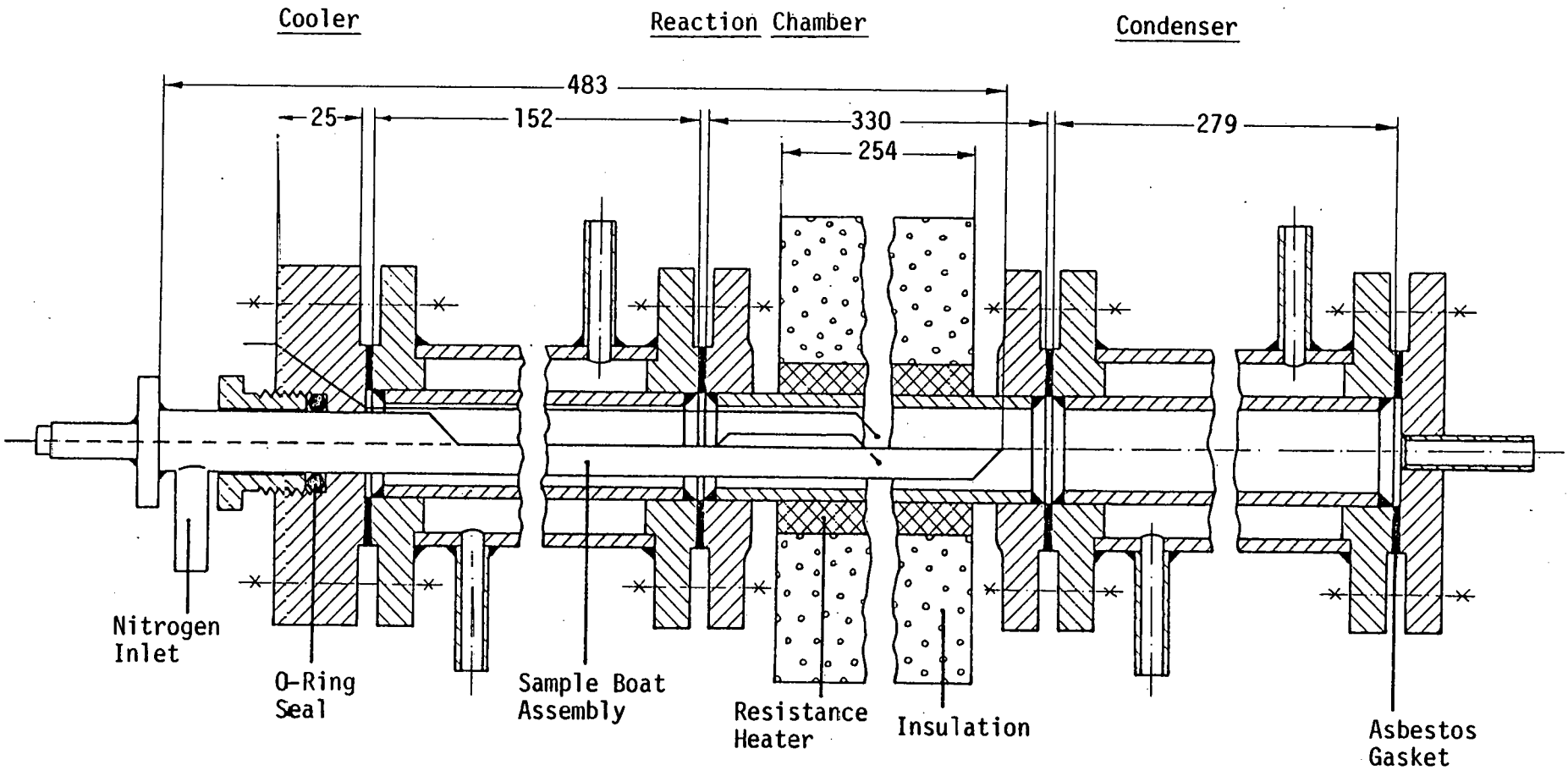

All Dimensions are in mm

Figure 4: Bench Scale Reactor - Details

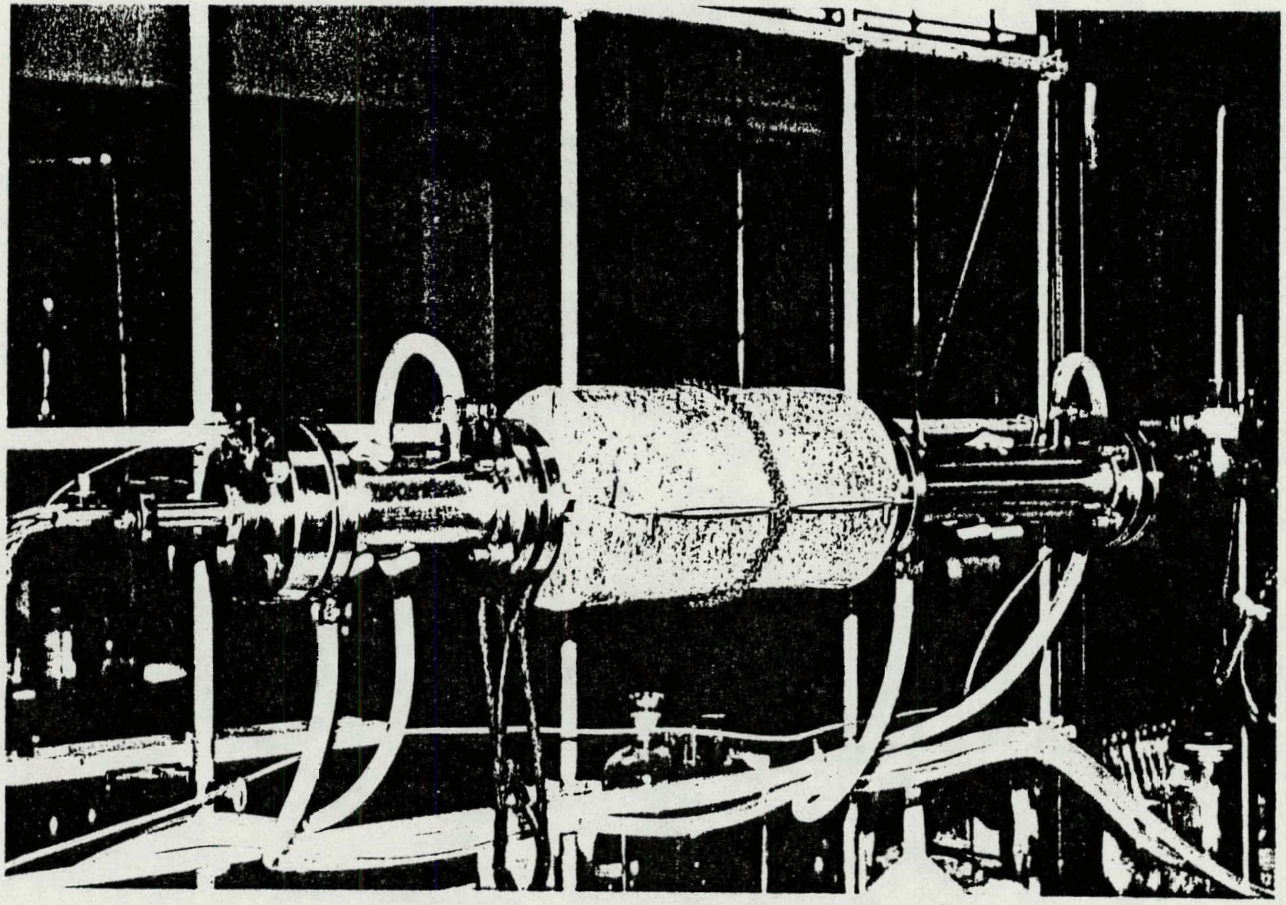

Figure 5: Bench Scale Reactor - Overall View

surrounded with 2 inches (51 mm) of insulation material. The temperature in the reaction chamber was measured with a stationary chromel-alumel thermocouple (TC 1) and controlled by a Thermo Electric Model 400 on-off proportional controller.

A sample boat assembly was used to insert the wood sample into the reaction chamber and to draw it back into the cooler at the end of a run without opening the reactor. The sample boat assembly was constructed of a 3/4 inch (19 mm), schedule 10, stainless steel tube, 19 inches (483 mm) long, the upper half of which was cut off to allow the sample boat to be moved on it. The sample boat assembly was sealed up at the upstream flange with an O-ring. A ceramic combustion boat 90 mm long and 14 mm wide was used as sample boat. A chromel-alumel thermocouple (TC 2) was positioned in the center of the sample boat in order to measure the reaction temperature accurately at the center of the sample. This thermocouple was also used to insert the sample boat into the reaction chamber and to remove it at the end of a run. Both thermocouples were connected to a Leeds & Northrup multipoint recorder Model 250. The temperatures were recorded every 3 seconds. The time constant of the thermocouples was determined to be 4.8 seconds.

The cooler was used to maintain the sample at a low temperature before it was inserted into the reaction chamber and to cool it down quickly at the end of a run. It was made of a 1 inch (25 mm) and a 2 inch (51 mm) schedule 40, stainless steel tube, 6 inches (152 mm) long. Tap water was used as cooling medium.

The purpose of the condenser was to condense and collect the tar. It was constructed in the same way as the cooler, but its length was 11 inches

(279 mm). Prior to each run the inside condenser wall was covered with aluminum foil and the interior space was loosely filled with steel wool.

Nitrogen supplied from a high pressure cylinder was used as inert gas. The nitrogen pressure was regulated by a two stage pressure regulator. The flow rate was controlled with a needle valve (V) and measured with a soap bubble meter.

The gas leaving the reactor was collected in a 18 liter plastic gas collection bag. The temperature of the gas stream was measured with a mercury thermometer (T2). The thermometer bulb was surrounded with some glass wool to allow a visual indication whether all tar was condensed in the condenser. A mercury manometer was used to check if the system is sealed up.

3.2 Operational Procedure

In each run a known amount of sawdust was charged into the ceramic sample boat and placed in the cooler. Thermocouple 1 was imbedded in the sample. Preweighed aluminum foil and steel wool were placed inside the condenser. The aluminum foil was carefully lined on the entire condenser walls and an edge of about 1-1/2 inches (38 mm) was extended into the reaction chamber to assure complete collection of the tar. The gas collection bag was thoroughly purged with helium to remove all the air and was then connected to the reactor outlet. The entire system was then checked for gas leaks by pressurizing it with nitrogen to two inches of mercury.

After the system was found to be free of leaks the heater and the temperature recorder were turned on and the setpoint was adjusted at the

temperature controller. The system was flushed with nitrogen during the entire heating-up period.

When the desired reactor temperature was reached and a steady state was achieved the flow rate was measured with the soap bubble meter (SM). The three way valve was turned to allow gas flow into the gas collection bag and the timer for the gas collection time was started. Then the sample boat was quickly inserted into the center of the reaction chamber by means of the embedded thermocouple and the timer for the reaction time was started.

When the desired reaction time expired the sample boat was withdrawn into the cooler. The nitrogen flow was continued for a few more minutes to purge the reactor and to assure that all gaseous products were collected in the gas collection bag. Then the three way valve was turned to allow gas flow to the atmosphere.

Both the reaction time and the time of gas collection were recorded. The weight of the residue in the sample boat and the weight increase of aluminum foil and steel wool were determined. The gas collection bag was disconnected from the reactor outlet and the gas was transfered to a 250 ml gas sampling bottle previously purged with helium. The gas was transfered from the gas collection bag by rolling it out completely through the gas sampling bottle. The gas sampling bottle was then isolated and labeled for later gas chromatographic analysis.

3.3 Analytical Procedure

3.3.1 Gas Analysis

The gas composition was determined for each run. Knowing the gas composition and the amount of nitrogen collected in the gas collection bag, the amount of gaseous products were calculated.

The collected gas was analyzed using a Carle Analytical Gas Chromatograph Model-AGC 111H connected to a Spectra-Physics Model Minigrator integrator. The gas chromatograph was equipped with 1/8 inch stainless steel columns packed as follows:

Column 1A	7' - 15% SF96 on Porapak P 50/80
Column 1B	8' - 15% SF96 on (75% Porapak N + 25% Porapak Q)
Column 2	5' - Molecular sieve 5A 42/60
Column 3A	4' - 20% Carbowax 1540 on Chromosorb T 40/60
Column 3B	6" - 15% SF96 on Porapak S 50/80
Column 4	6' - 8% OV 101 on Chromosorb W-AWDMCS 80/100

Helium was used as carrier gas. The Carle AGC-111H gas chromatograph was equipped with dual filament thermal conductivity detectors. The sample was injected by a mini-valve the actuation of which was controlled by a Carle Series-S Mini Valve Programmer. Before using the gas chromatograph,it was calibrated with a gas mixture of known composition.

Helium is a favorable carrier gas for all components except hydrogen when a thermal conductivity detector is used. Helium and hydrogen have very similar thermal conductivities, and measuring hydrogen in a helium environment gives low sensitivity, nonlinearity, and troublesome peak reversals. Therefore, the Carle AGC-11H gas chromatograph was equipped with a Hydrogen Transfer System (HTS) which enabled us to measure hydrogen concentration without any difficulty. After measuring all components except hydrogen, hydrogen was transfered by the HTS into a nitrogen carrier gas before measurement.

3.3.2 Elemental Analysis

Elemental analysis of tar and char were carried out to determine their nitrogen, carbon, hydrogen, and oxygen content at various reactor temperatures. The analysis was performed with a Perkin-Elmer Elemental Analyzer Model 240B. It determined the carbon, hydrogen, and nitrogen content of organic compounds by converting the sample into carbon dioxide, water and nitrogen by means of combustion. The sample combustion occurred in pure oxygen at 975°C. Helium was used to carry the combustion products from the combustion train through the analytical system. The combustion products were analyzed in a self-integrating thermal conductivity analyzer.

For oxygen analysis the sample is pyrolyzed in helium at 975°C, over platinized carbon, and then the produced oxygen is converted to carbon monoxide. The carbon monoxide and the remaining gases pass through copper oxide packing at 670°C where the carbon monoxide is converted to carbon dioxide. The readout of the C-detector is then recorded and the oxygen analysis is complete. The results are displayed in a bar graph form on a 1 mV recorder.

The sample size for elemental analysis was 1 to 3 mg. It was determined with a Cahn Electrobalance Model G.

3.3.3 Thin Layer Chromatography

Thin layer chromatography analysis for the tar were done to get a qualitative impression about the tar composition. The analysis was performed on silica gel eluted with a mixture 1:1 methyl ethyl ketone-chloroform; carbohydrates were detected by using iodine.

3.4 Feed Material

The pyrolysis of Missouri oak sawdust was studied in this investigation. The particle size distribution of the as-received sawdust is shown in Figure 6. The surface-average particle size was 0.840 mm. Visual observation suggested that the particles had cylindrical shape. The bulk density was determined by Wang (2) to be 0.25 g/cm^3.

Before the sawdust was pyrolyzed it was dried at 120°C for one hour and then screened. Figure 7 shows the drying curve of sawdust. It is evident that a drying time of one hour was sufficient to drive off all the moisture in the wood. The particle size distribution of the dried sawdust is shown in Figure 8. The surface-average particle size was 0.615 mm. The difference between the mean diameter of dry and as-received wood particles was probably due to shrinking of the particles occurred during the drying. An elemental analysis performed on the dried sawdust indicated that the wood contained 47.0% C, 5.6% H and 41.8% O (weight percent).

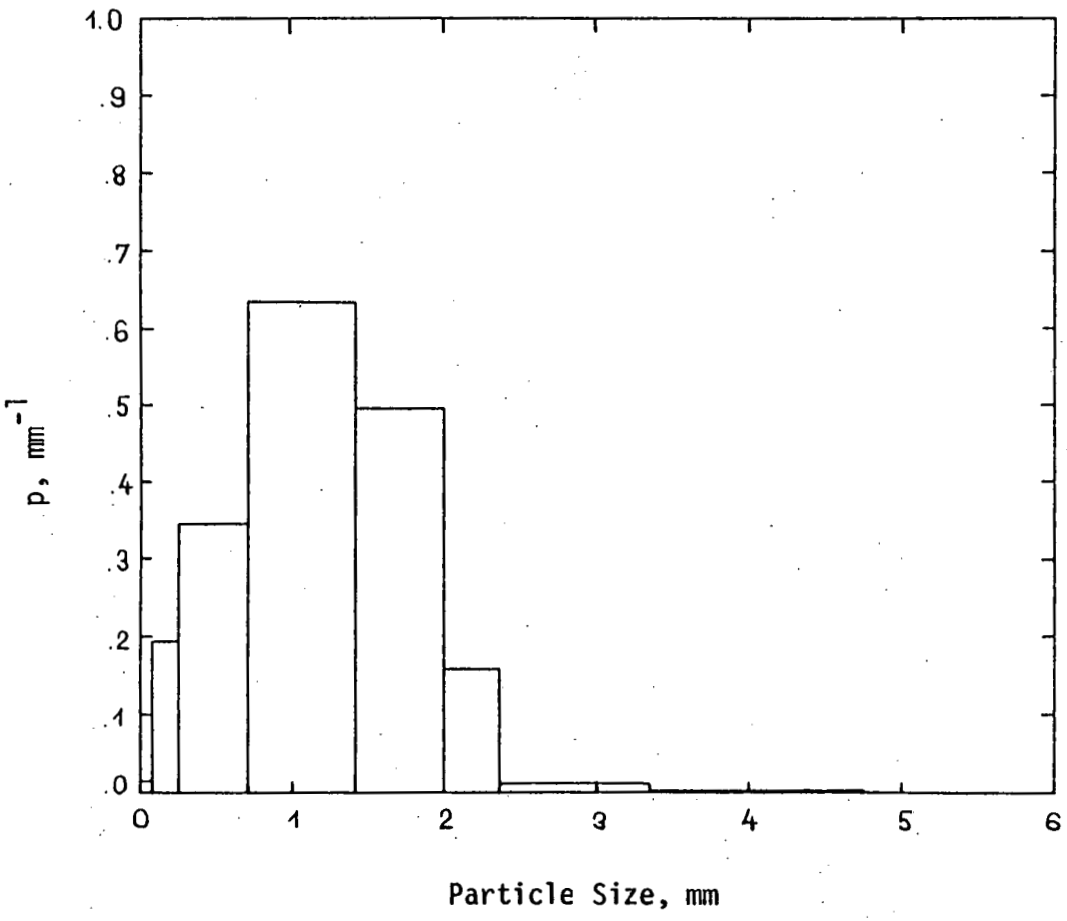

Figure 6: Particle Size Distribution of As-Received Sawdust

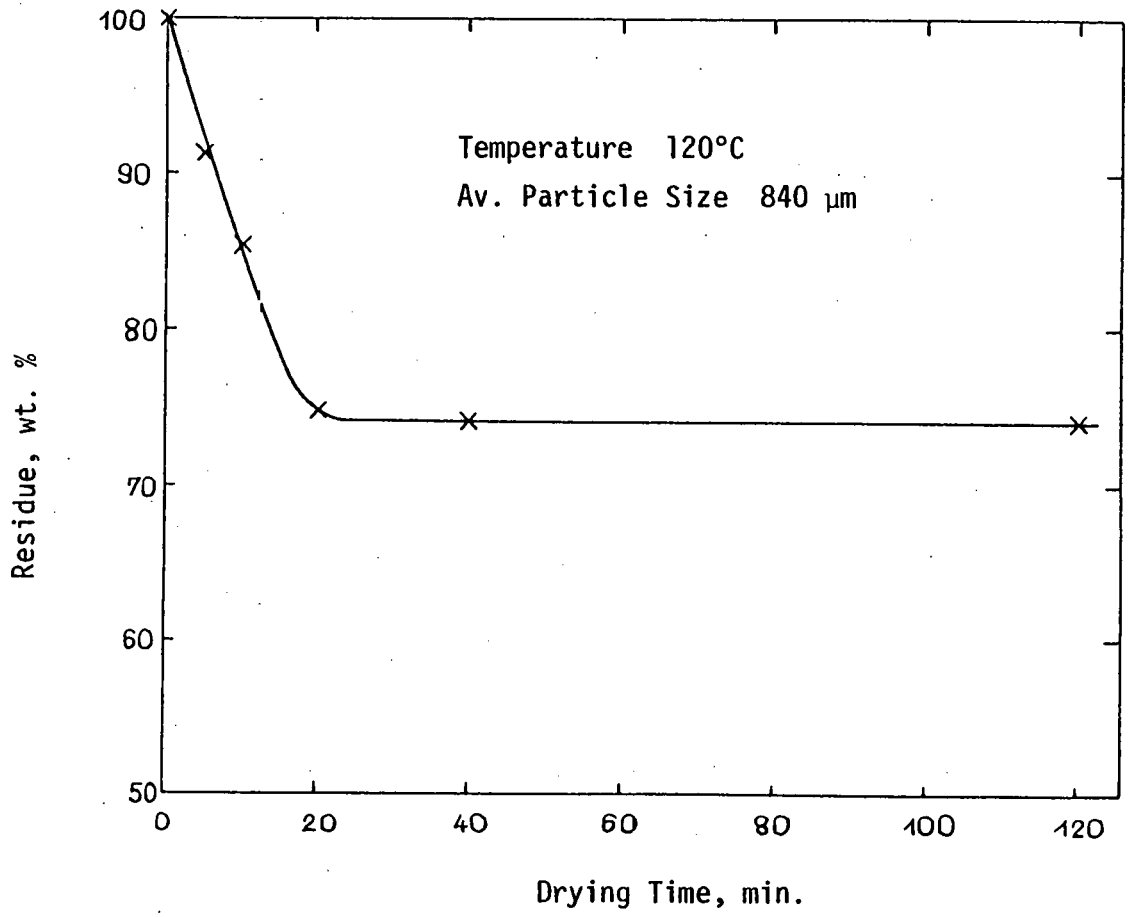

Figure 7: Drying Curve of Sawdust

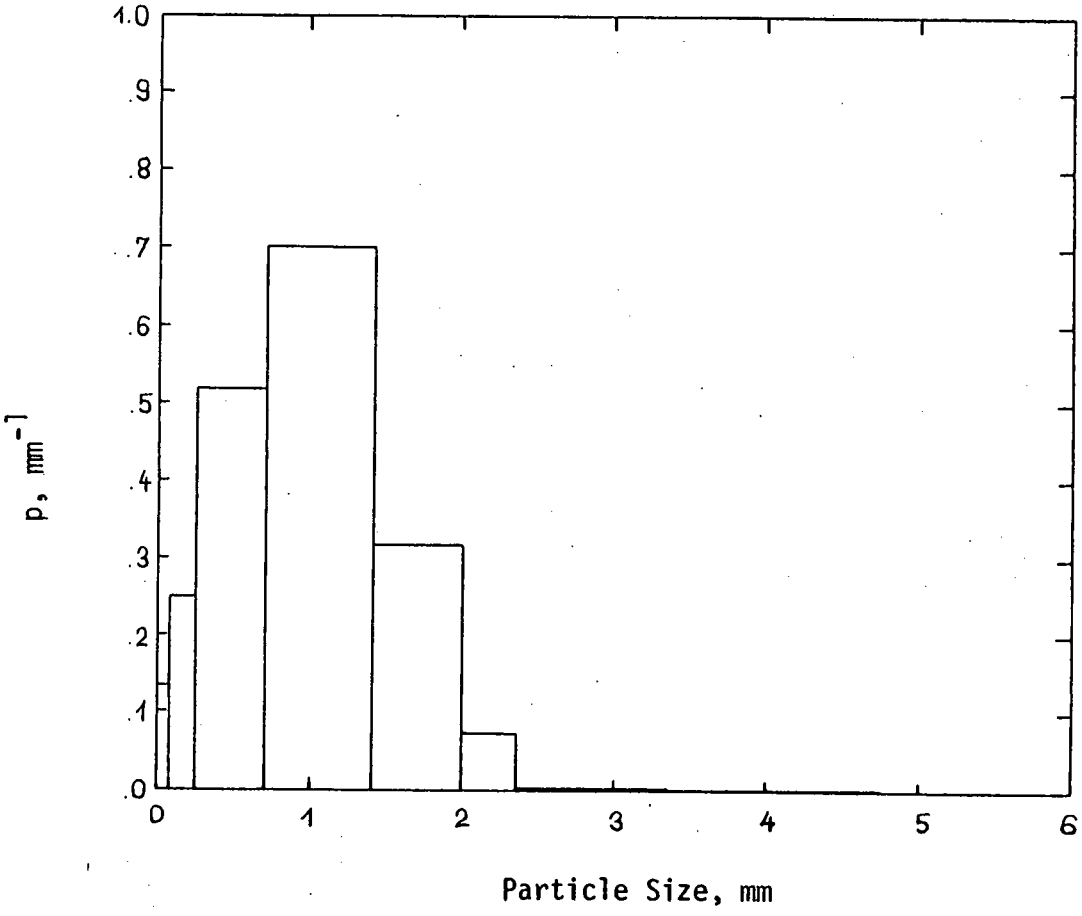

Figure 8: Particle Size Distribution of Dried Sawdust

4. DISCUSSION OF RESULTS

This chapter summarizes the experimental results and provides an analysis and discussion of these results. The first part deals with the influence of transport effects on the wood pyrolysis. The second part concerns with the determination of the kinetic parameters of wood pyrolysis. In the last part the analysis of the pyrolysis products is discussed. The experimental data are tabulated in Appendices A and B.

4.1 Influence of Transport Effects

The pyrolysis of wood is a chemical reaction coupled with transport of heat and mass. In order to explain the various steps of heat and mass transfer occurring during wood pyrolysis we consider a sample which consists of several wood particle layers placed in a stream of inert gas and exposed to higher temperatures. The individual wood particles are composed of a lot of small cellulosic cells.

Let us focus our attention on one particle in the sample. In order to provide the appropriate energy and temperature necessary for the decomposition of the cell heat must be transported from the bulk stream to the cell inside this particle. The thermal decomposition of the cellulosic cell is the chemical reaction which we want to investigate. Simultaneously, the reaction products are transported out of the particle through the void between the particles to the bulk stream.

Assuming that the energy and temperature for the decomposition of the cell inside the particle is available the total process of wood pyrolysis probably occurs in the following steps (see Figure 9):

(1) thermal decomposition of the cellulosic cell,

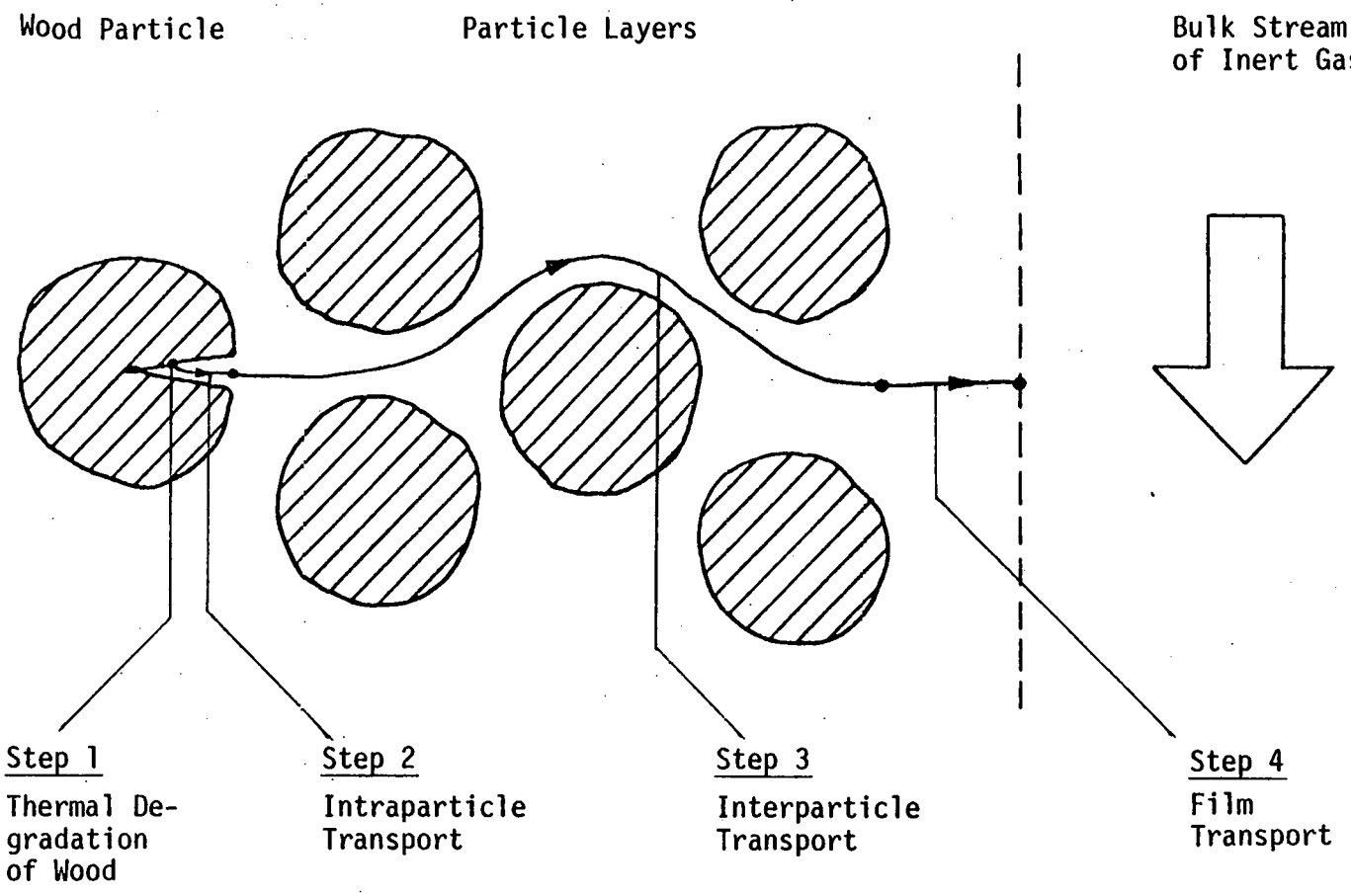

Figure 9: Illustration of Transport Effects During Wood Pyrolysis

(2) intraparticle transport of the reaction products,

(3) interparticle transport of the reaction products, and

(4) film transport of the reaction products.

The heat transfer can be divided in similar steps as the mass transfer, they occur only in reverse direction.

Within the scope of the total process the pyrolysis may be regarded as a series of steps("resistances")where the slowest step determines the rate of the whole process. To determine the intrinsic kinetics of wood pyrolysis it is convenient to conduct the experiments under conditions under which the chemical reaction is rate-controlling step. Therefore preliminary experiments were carried out to determine the conditions under which the chemical reaction is the controlling step.

4.1.1 Effect of Film Transport

In order to examine the effect of film transport several runs were conducted at different nitrogen flow rates. When the film transport is the rate-controlling step the overall reaction rate should increase as the flow rate increases. The reactor temperature was 450°C that is higher than the temperature range in which the pyrolysis kinetic was investigated (300 to 400°C). If the chemical reaction is the controlling step at 450°C it will be in any case the controlling step at lower temperature. The sample weight loss over a 10 min. reaction time was selected as a measure for the reaction rate. Figure 10 illustrates that for nitrogen flow rates in the range of 1 to 5 ml/sec the sample weight loss is independent of the nitrogen flow rate. Therefore, it can be concluded that the film transport is not a rate-controlling step.

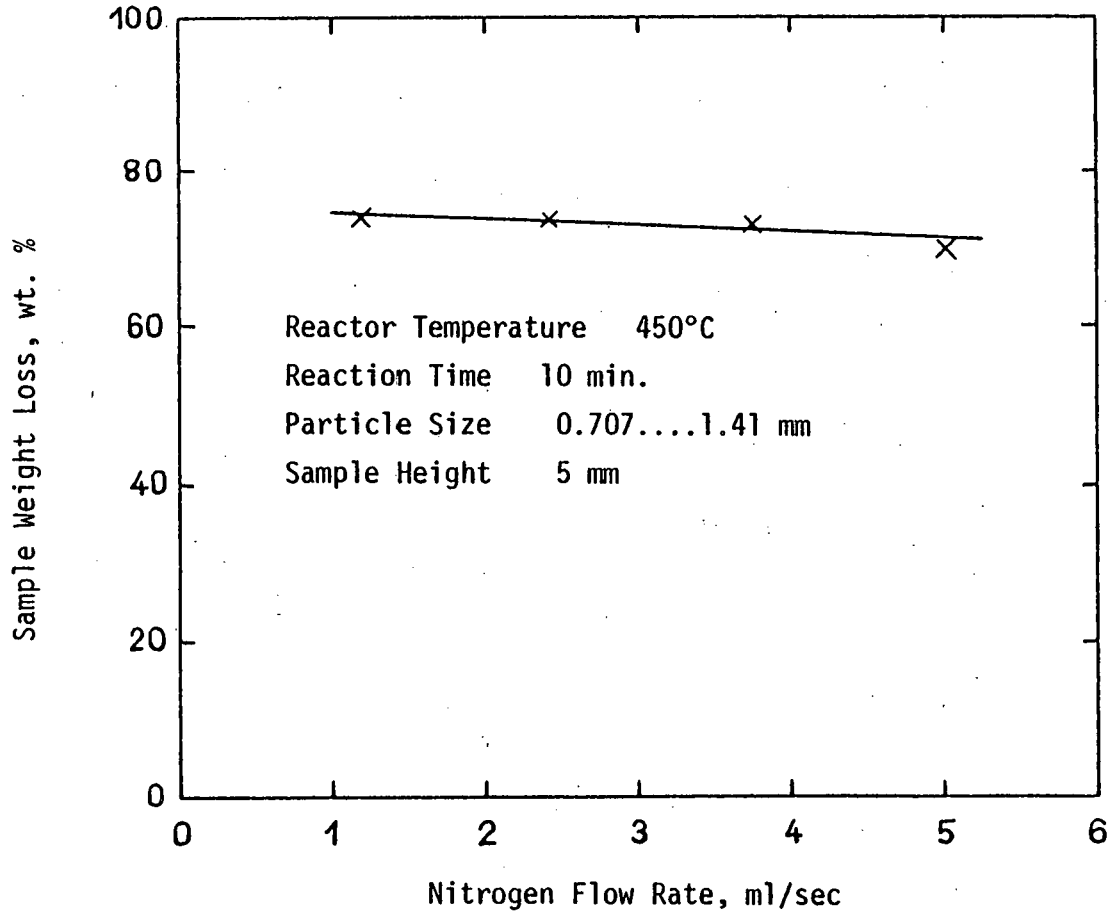

Figure 10: Influence of Film Transport

4.1.2 Effect of Interparticle Transport

The effect of interparticle transport was studied by measuring the sample weight loss for different sample heights. The "resistance" of interparticle transport depends on the length of the transport path which is in our case identical to the sample height. If the overall reaction rate decreases as the sample height increases interparticle transport is the rate-controlling step. The weight loss was measured for sample heights of 1.5, 3, 4.5, and 6 mm. Figure 11 shows that the sample weight loss is independent of the sample height and consequently the interparticle transport is not the rate-controlling step.

4.1.3 Effect of Intraparticle Transport

The transport effects inside the particles were investigated by measuring the sample weight loss for different particle sizes. When intraparticle transport is the rate-controlling step the overall reaction rate increases as the particle size decreases. In this investigation, the average particle size was varied in the range 0.037...2.180 mm. Figure 12 illustrates that the sample weight loss is independent of the particle size in the investigated range. The intraparticle transport is, therefore, not the rate-controlling step.

The foregoing results show that for temperatures below 450°C, wood particles smaller than 2 mm and nitrogen flow rates higher than 2 ml/sec the chemical reaction is the controlling step. This is in agreement with the measurements on a single wood particle done by Maa (10, 11). In this study the kinetic of wood pyrolysis was, therefore, determined in the range of 300 to 400°C, with wood particles of about 1 mm and at a nitrogen flow rate of about 3.5 ml/sec.

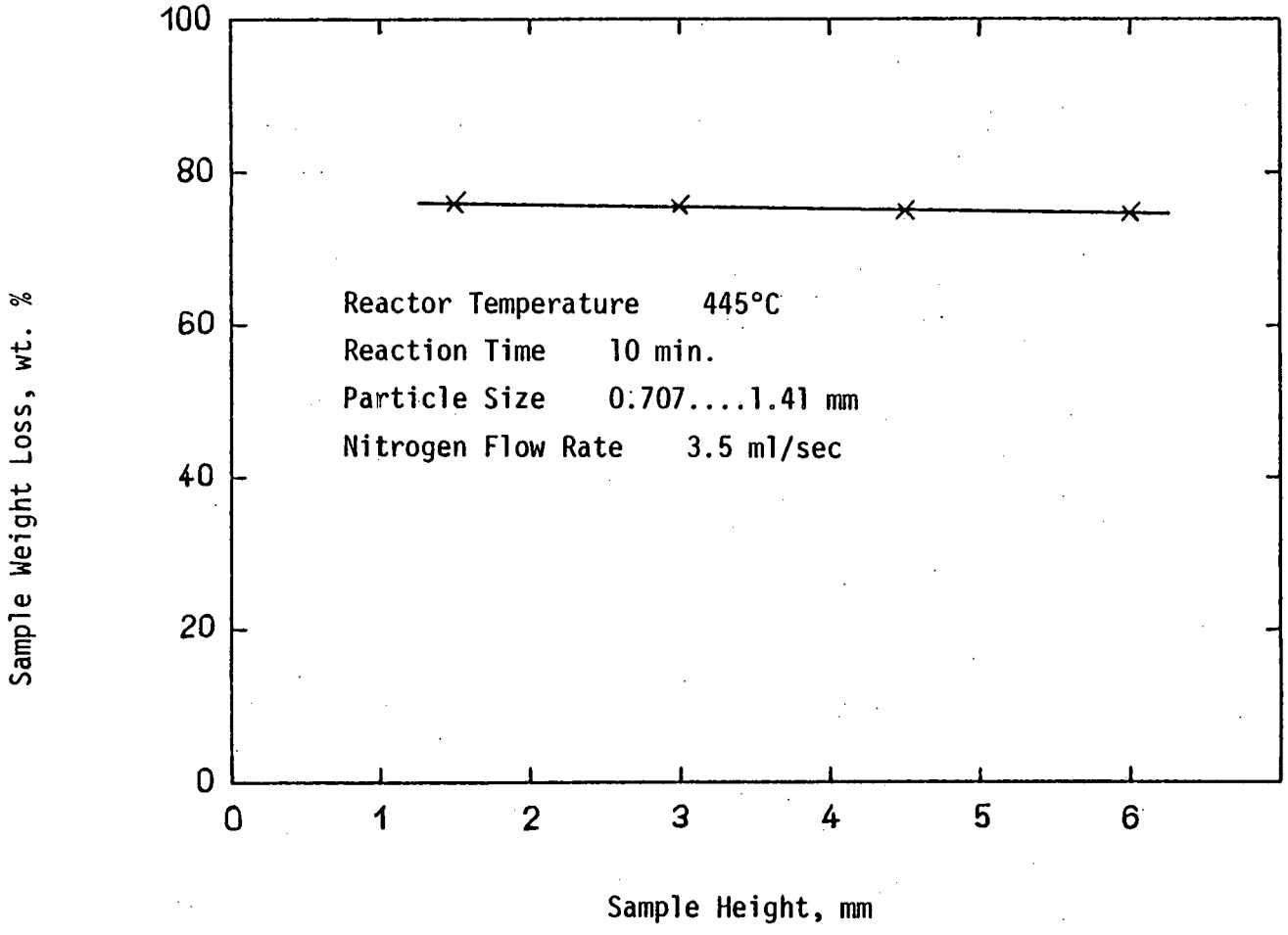

Figure 11: Effect of Interparticle Transport

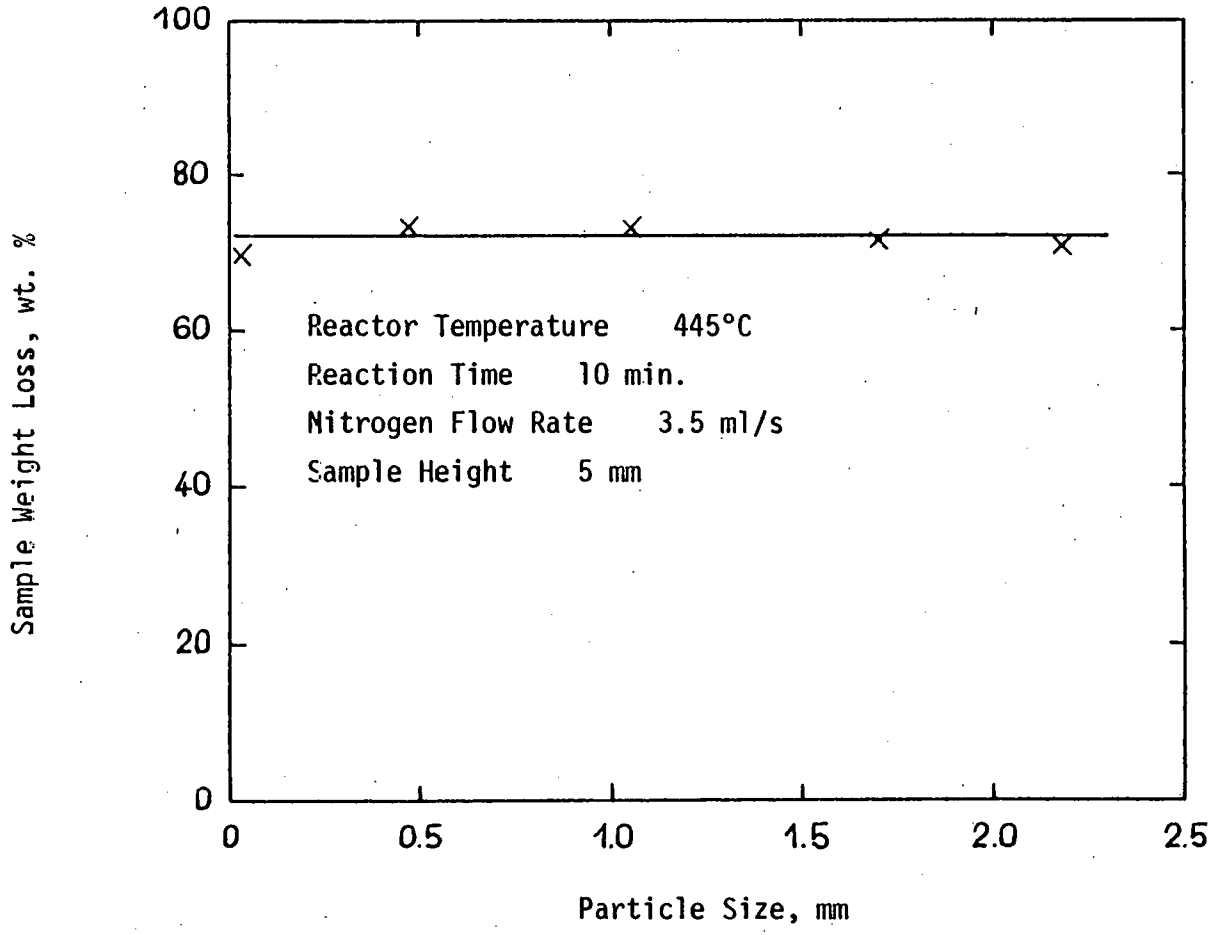

Figure 12: Effect of Intraparticle Transport

Figure 13 illustrates qualitatively the relative importance of chemical reaction and transport effects at different reactor temperatures. Photographs of two cross sections of pyrolyzed wood particles are shown. Two cylindrical wood particles with initial diameter of about 12 mm were pyrolyzed one at 550°C for 20 seconds and the other at 349°C and 5 min. The left photograph shows that for the low temperature the reaction took place throughout the whole particle. The conversion of the particle shown was about 40%. In this case the chemical reaction was the rate-controlling step. The right photograph illustrates that at 550°C the reaction occurred in a small peripherial zone. At that temperature the transport steps were rate-controlling because the increase of the chemical reaction rate was higher than the increase of the transport rate.

4.2 Determination of Kinetic Parameters

The kinetic parameters of wood pyrolysis were determined from measurements of the mass fraction of residue, tar, and gas as a function of reaction time at three reactor temperatures: 354, 369, and 392°C (see Figures 14, 15 and 16). In order to get an idea about the accuracy of the measurements an overall material balance was calculated for each run. A 5 percent agreement was achieved in most runs. The experimental points are marked in the figures and the drawn curves represent the best visual fit of the experimental data. The dashed curve indicates the reaction temperature measured with the thermocouple embedded in the sample (TC 2 in Figure 3).

The reaction rate constants k_1, k_2 and k_3 were determined according to the procedure described in Chapter 1 and depicted in Figure 2. As

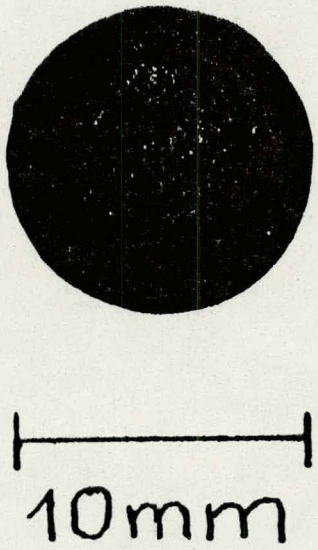

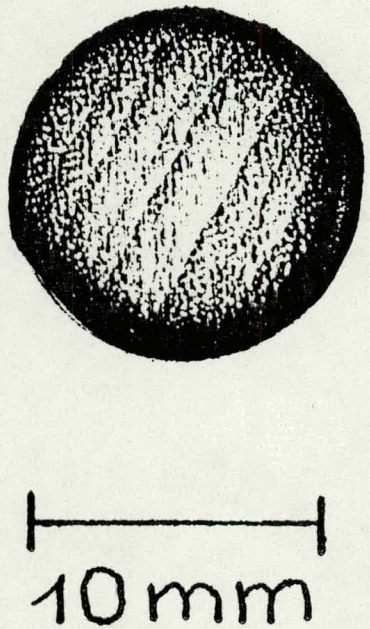

Reactor Temperature, 349°C
Reaction Time, 5 min.

Reactor Temperature, 550°C
Reaction Time, 20 sec.

Figure 13: Photographs of Cross Sections of Single Particles

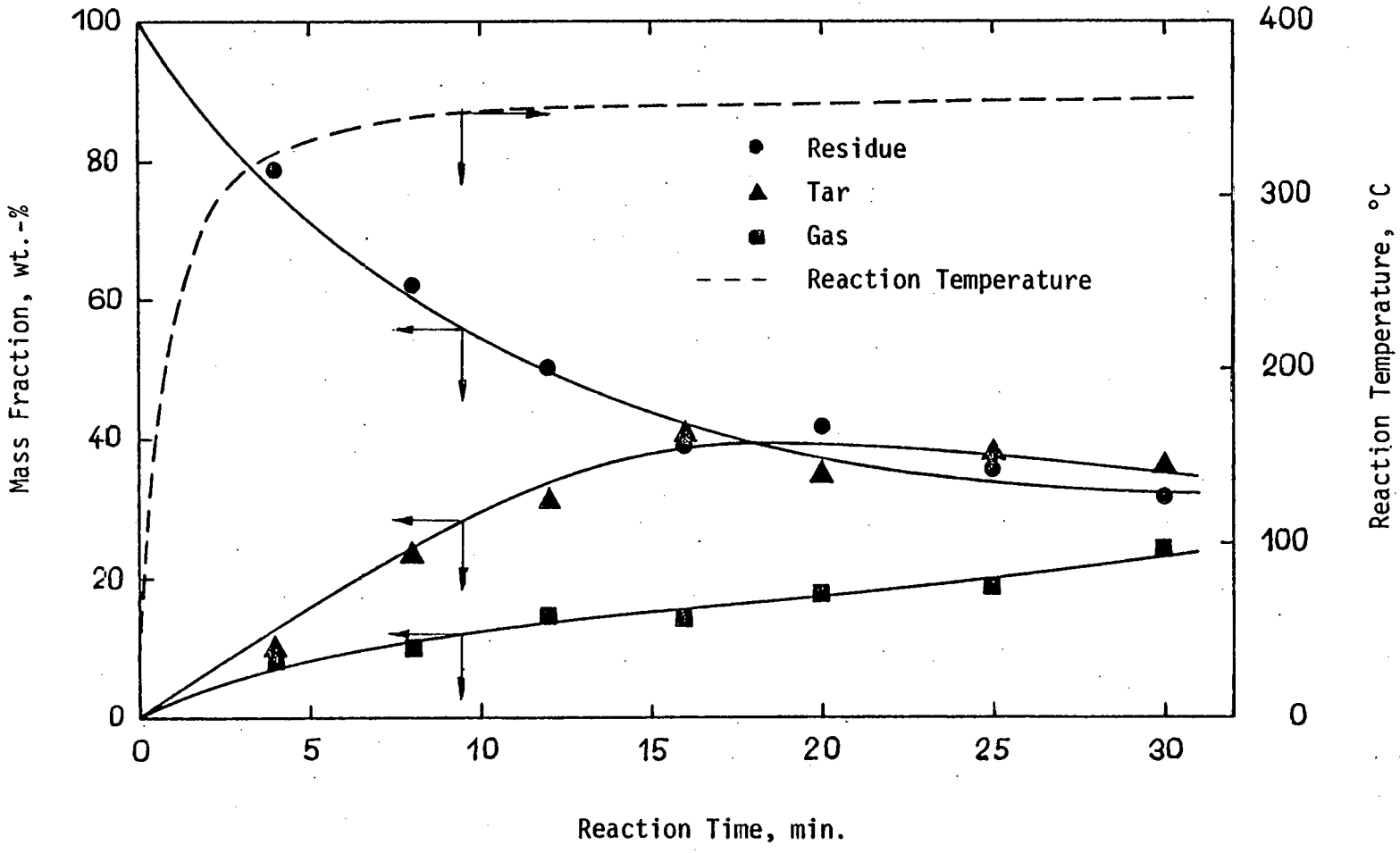

Figure 14: Composition-Time Curves, Reactor Temperature 354°C

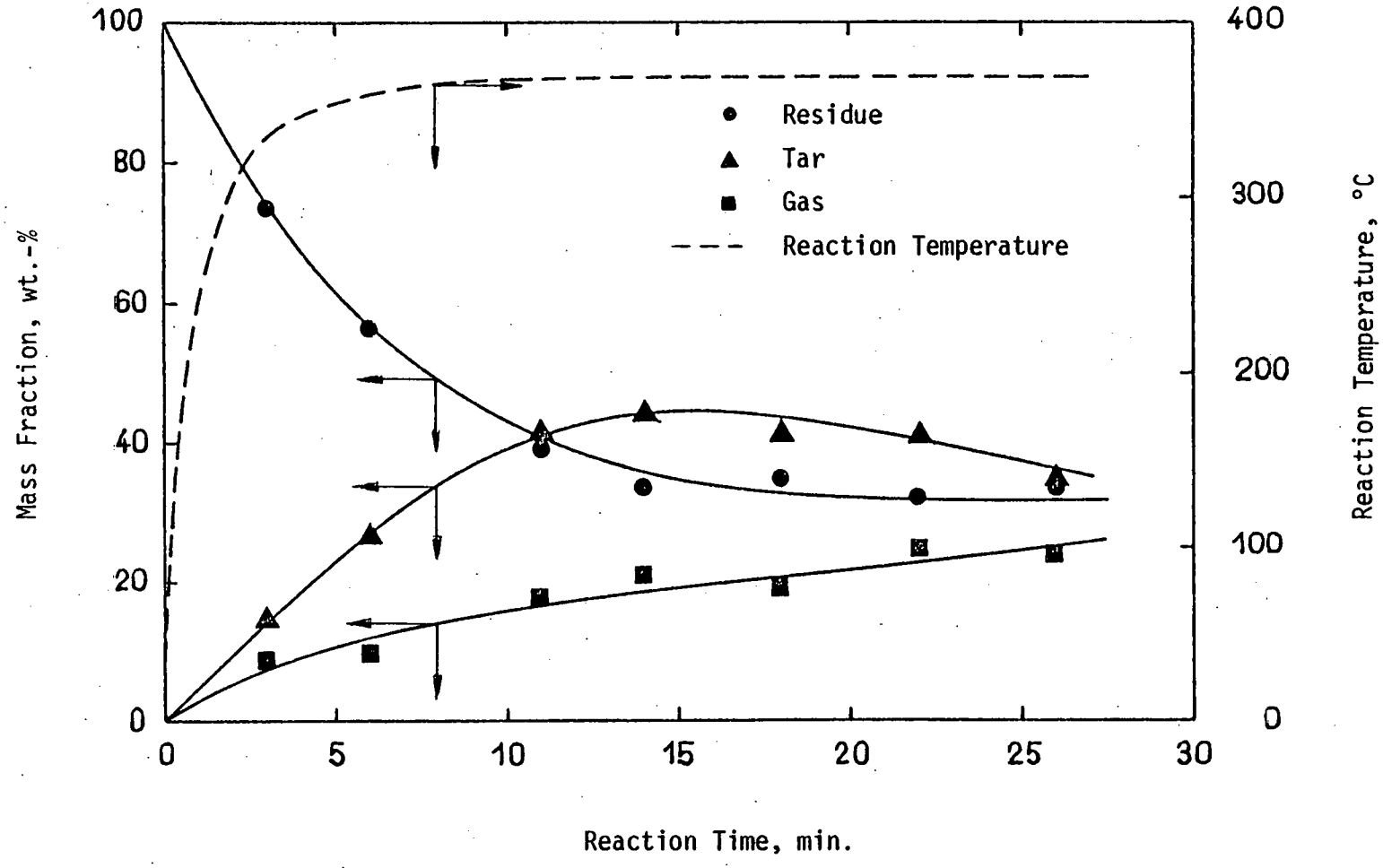

Figure 15: Composition-Time Curves, Reactor Temperature 369°C

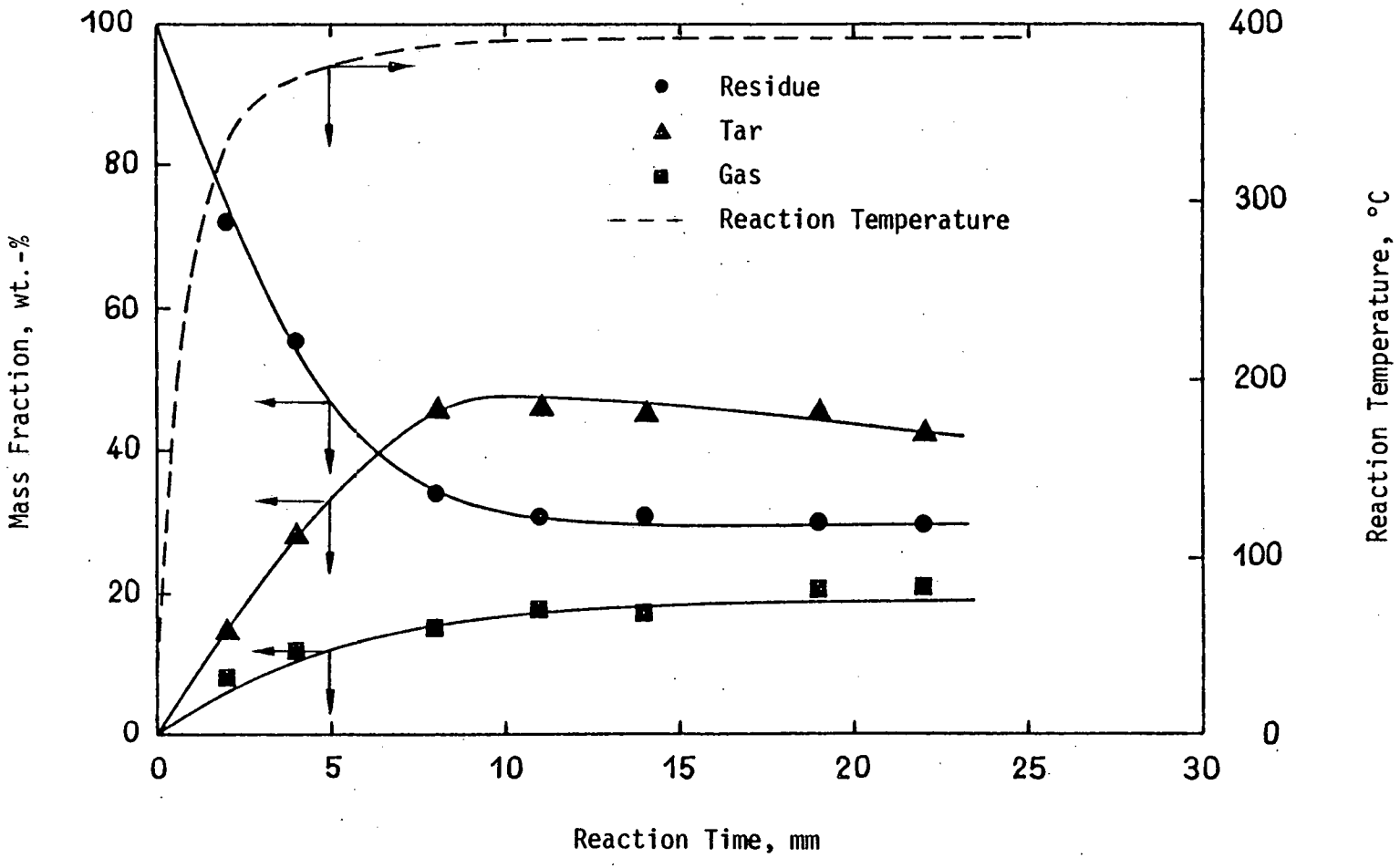

Figure 16: Composition-Time Curves, Reactor Temperature 392°C

indicated there these relations can be used even for non-isothermic conditions when $k_3/(k_1 + k_2)$ is independent of the temperature. This was examined by measuring $w_R(t \to \infty)$ at reactor temperatures of 329, 354, 369 and 392°C. The value of $w_R(t \to \infty)$ was determined by measuring the residue mass fraction for complete conversion. Complete conversion was assumed, when the weight loss of residue was less than 0.5 percent over a period of 30 min. The mean value of the measured $w_R(t \to \infty)$ was 0.299 and its standard deviation was 0.028. This suggested that the assumption $k_3/(k_1 + k_2)$ is independent of the temperature is justified.

In determining the reaction rate constants from the experimental data two points should be considered: First, Atika (17) showed that kinetics data for the pyrolysis of cellulosic materials obtained above 340°C were different from those obtained at lower temperature. Therefore, in this investigation the kinetic parameters were determined from the experimental data at reaction temperatures above 325°C. Second, a small amount of the tar was condensed on the aluminum foil placed in the downstream end of the reaction chamber. This tar was decomposed at long reaction times according to the secondary steps (see 2-1). Hence the kinetic parameters were determined between 3 and 10 min, to avoid the secondary steps.

The reaction rate constants k_1, k_2 and k_3 were calculated for seven different reaction temperatures in the range 325 to 385°C. The Arrhenius plot of these data is shown in Figure 17. Slopes and intercepts were determined by linear regression. Table 2 gives activation energies and frequency factors of the three primary reactions and the overall pyrolysis reaction. The activation energy for reaction (1 + 2) is somewhat lower as the range of 109 to 139 kJ/mol reported by other investigators (8, 12,

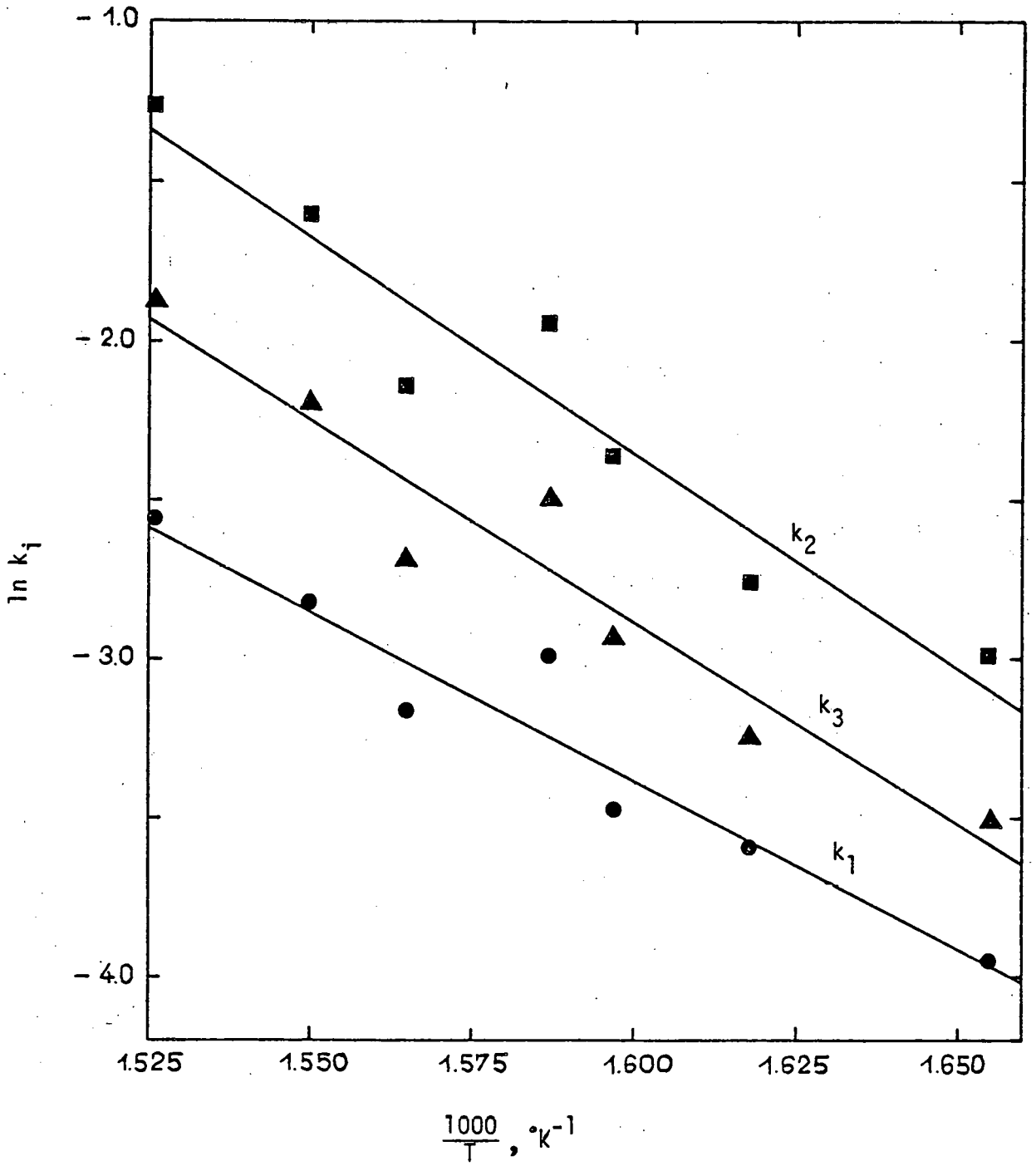

Figure 17: Arrhenius Plot of Reaction Rate Constants

Table 2: Frequency Factors and Activation Energies

Reaction	Frequency Factor	Activation Energy	90% Confidence Interval for Activation Energy	Correlation Coefficient
——	min^{-1}	kJ/mol	kJ/mol	——
k_1	8.607×10^5	88.6	$\pm$ 23.1	-0.96
k_2	2.475×10^8	112.7	$\pm$ 29.8	-0.95
k_3	4.426×10^7	106.5	$\pm$ 27.2	-0.96
$k_1 + k_2$	1.039×10^8	106.5	$\pm$ 27.4	-0.96
k	1.481×10^8	106.5	$\pm$ 27.4	-0.96

13, 14, 15). The reason of the wide variation of activation energies found by the other investigators is probably due to inaccurate temperature measurement. The activation energies for the three primary steps are comparable. That means that the distribution of the pyrolysis products is not largely dependent on the reaction temperature in the temperature range investigated.

To evaluate whether the kinetic parameters calculated above can be used to predict the yield of the pyrolysis products, the composition-time curves were computed by using these kinetic parameters. In principle, it is possible to calculate the cumulative mass fraction of component i as a function of time by

$$w_i(t) = \int_0^t \left(\frac{dw_i(\theta)}{d\theta}\right) d\theta \quad , \tag{4-1}$$

where i stands for W, G, T, and C and the $dw_i(\theta)/d\theta$ are given by (2-2) to (2-5). In the integration the variations of the kinetic rate constants with time should be taken into consideration. This is done by using the temperature time curve. In practice, it is not possible to solve this set of equations analytically. Therefore, a numerical integration was carried out. The differential equations (2-2) to (2-5) were converted into difference equations.

$$\frac{\Delta w_W(t)}{\Delta t} = (k_1 + k_2 + k_3) w_W(t) \tag{4-2}$$

$$\frac{\Delta w_G(t)}{\Delta t} = k_1 \, w_W(t) \tag{4-3}$$

$$\frac{\Delta w_T(t)}{\Delta t} = k_2 w_W(t) \qquad (4\text{-}4)$$

$$\frac{\Delta w_C(t)}{\Delta t} = k_3 w_W(t) \qquad (4\text{-}5)$$

These equations were solved numerically by using small time increments. The calculated composition-time curves were then compared with the experimental data. The curves did not predict well the experimental data especially during the heating-up period. Roberts (12) reported that the mechanism of wood pyrolysis above 340°C is different from the mechanism at lower temperatures. This is probably the reason for the deviations of all curves during the heating-up period.

In another attempt, the composition-time curves were calculated by relation (2-10) to (2-13) and using the temperature achieved for the thermal steady state, which will be referred to as reactor temperature. In this case the conversion during the heating-up period was, as expected, higher than the experimental conversion, since the actual reaction temperature was much lower than the final reaction temperature used.

At this point it was decided to check whether the experimental composition-time curves can be predicted by using (2-10) to (2-13) with some constant temperature. The problem was to find a proper reaction temperature to be used. The temperature is an empirically determined average reactor temperature. We tried to use an integral-mean temperature,

$$\bar{T} = \frac{1}{t} \int_0^t T(\theta)\, d\theta, \qquad (4\text{-}6)$$

and found that the best fit was achieved when using for t in (4-6) the

reaction time for 97 percent conversion. The calculated composition-time curves are shown in Figures 18, 19, and 20. The predicted curves agree quite well with the experimental data. Only for long reaction times the experimental values for the tar composition were lower than calculated. The reason for this is, as explained before, the decomposition of the tar condensed in the downstream edge of the reaction chamber. This method for the calculation of the composition-time curves represents an improvement over the common practice of using the final reaction temperature, since it takes into account the heating-up period.

4.3 Analysis of the Pyrolysis Products

4.3.1 Gas

For each run a gas chromatographic analysis of the collected gas was carried out. The gas composition was used to calculate the product gas yield by using nitrogen balance. The influence of reaction time and reactor-temperature on the gas composition were investigated. The nitrogen-free product gas obtained in this investigation consisted mainly of carbon dioxide, carbon monoxide, oxygen, and C_3^+ - compounds. No attempt was made to identify the individual compounds of the C_3^+ - fraction. Trace amounts of acetylene, ethylene, and methane were detected.

A relatively large amount of oxygen has been measured in the product gas especially at low reaction times. This differs from the gas compositions obtained by other investigators (15, 18, 19). They did not indicate the presence of oxygen in the product gas. In this study precautions were made to prevent oxygen penetration into the experimental system (see Section 3.3). The oxygen content obtained in a blank run was negligible.

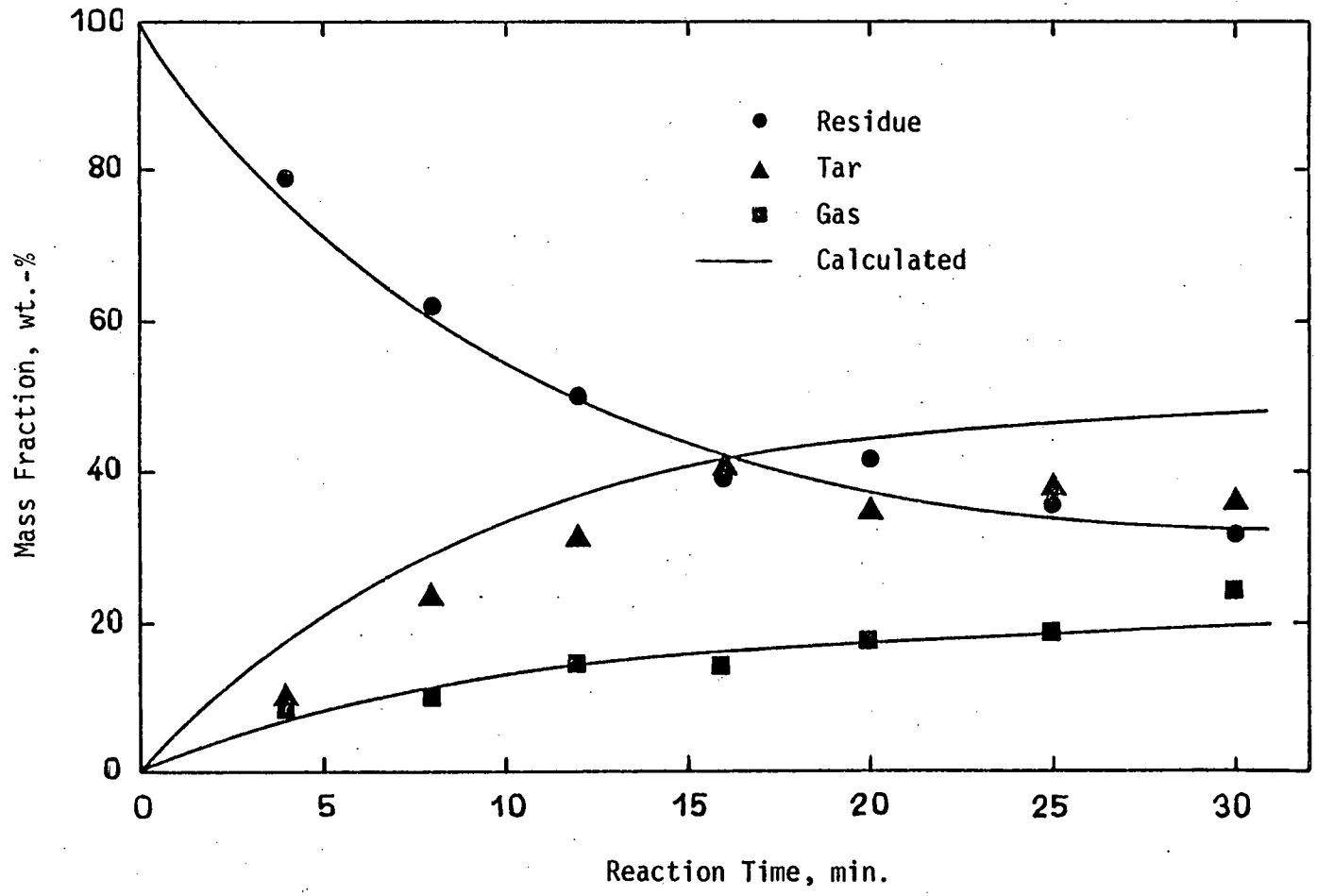

Figure 18: Comparison between Experimental and Calculated Results, Reactor Temperature 354°C

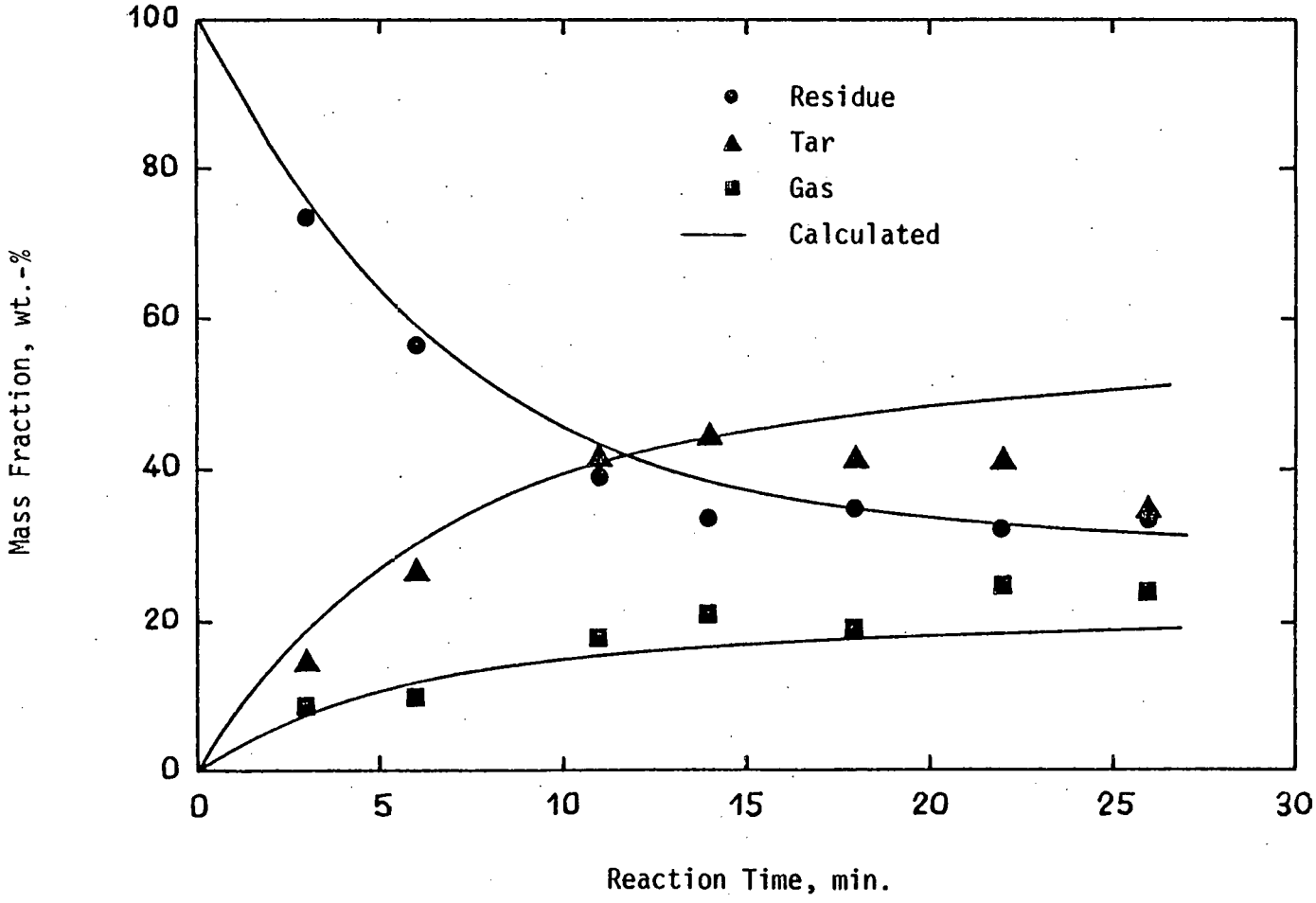

Figure 19: Comparison between Experimental and Calculated Results, Reactor Temperature 369°C

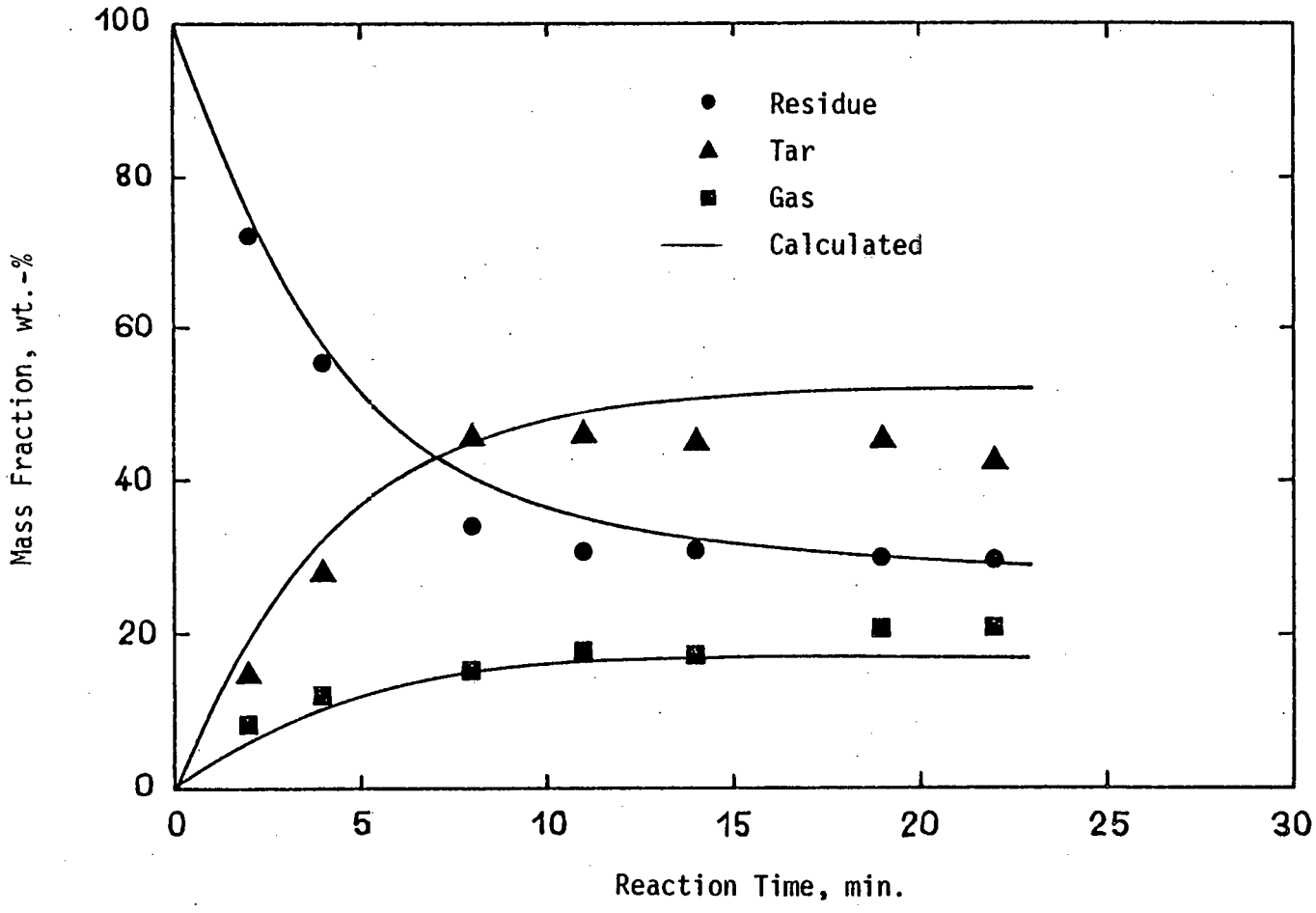

Figure 20: Comparison between Experimental and Calculated Results, Reactor Temperature 392°C

However, it should be noted that the total amount of oxygen analyzed in the product gas was only 20 to 30 mg. Perhaps, the source of the oxygen was oxygen absorbed on the sample surface prior to each run.

The gas composition as a function of reaction time at three different reactor temperatures are shown in Figures 21, 22 and 23. The gas composition is expressed in cumulative volume percent which is the composition over the entire period. The figures show that for each reactor temperature the amount of carbon dioxide and carbon monoxide in the product gas have a maximum which occurred at higher reactor temperatures at low reaction times. Determination of the reaction temperatures at which the maximums occurred showed that they appeared between 360 and 390°C. Examining TGA curves for wood and cellulosic material reported by other investigators revealed that maximum weight loss was measured in this temperature range (3, 9, 18, 19). We believe that carbon dioxide and carbon monoxide are produced by decarboxylation in this temperature range. At lower temperatures mainly gradual depolymerization of cellulose takes place. The depolymerization does not yield carbon dioxide and carbon monoxide. The figures also indicate that the amount of C_3^+ - compounds increased with increasing temperature. No definite explanation for this can be given at this time.

Figure 24 shows the gas composition obtained for high conversion at different reactor temperatures. Carbon monoxide content increases with increasing reactor temperature. This is probably due to the increase of decarboxylation at high temperature. Carbon dioxide content has a minimum around 369°C whereas C_3^+ has a maximum around the same temperature. The latter is probably because at lower temperatures the energy required for

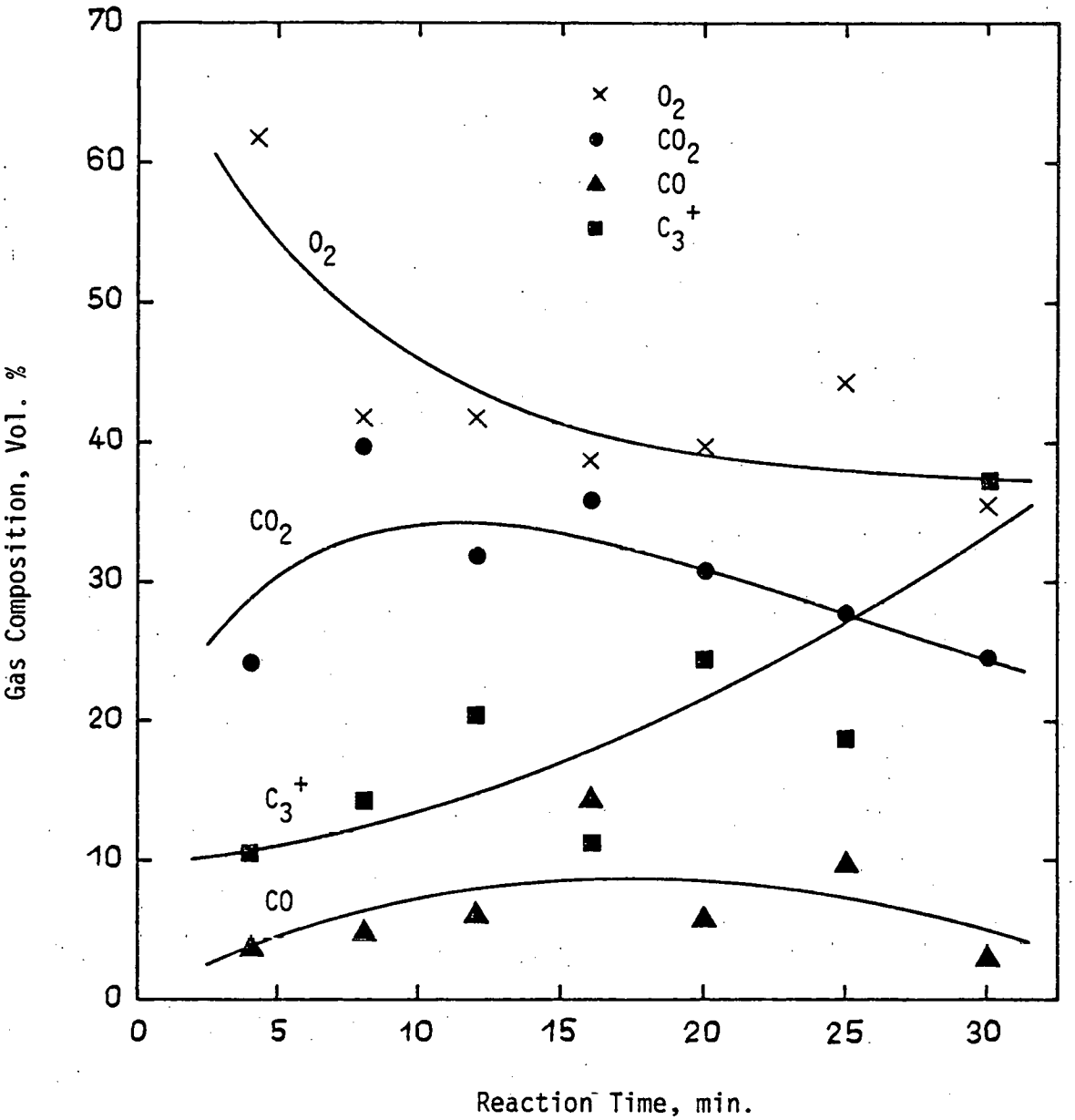

Figure 21: Gas Composition, Reactor Temperature 354°C

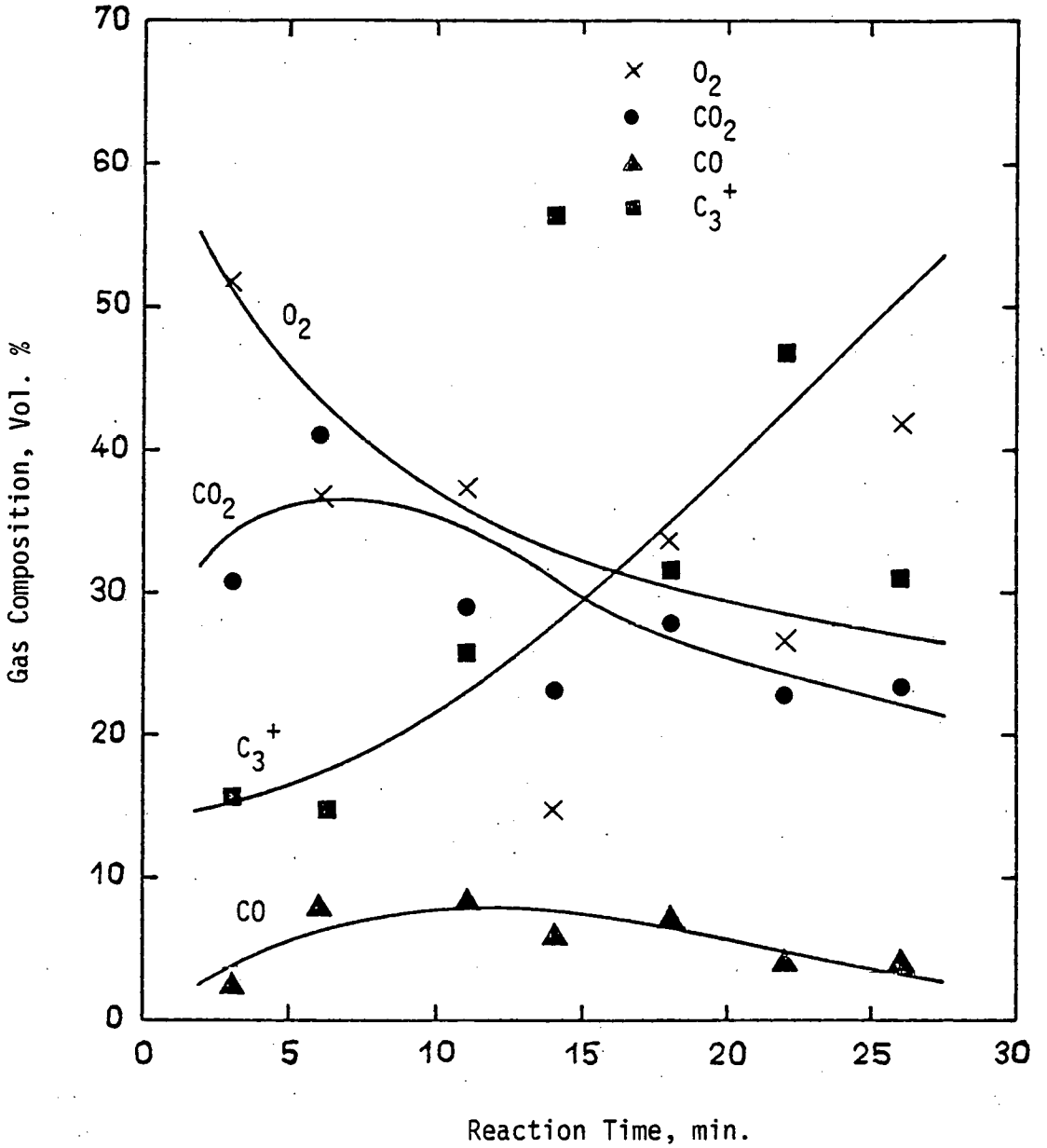

Figure 22: Gas Composition, Reactor Temperature 369°C

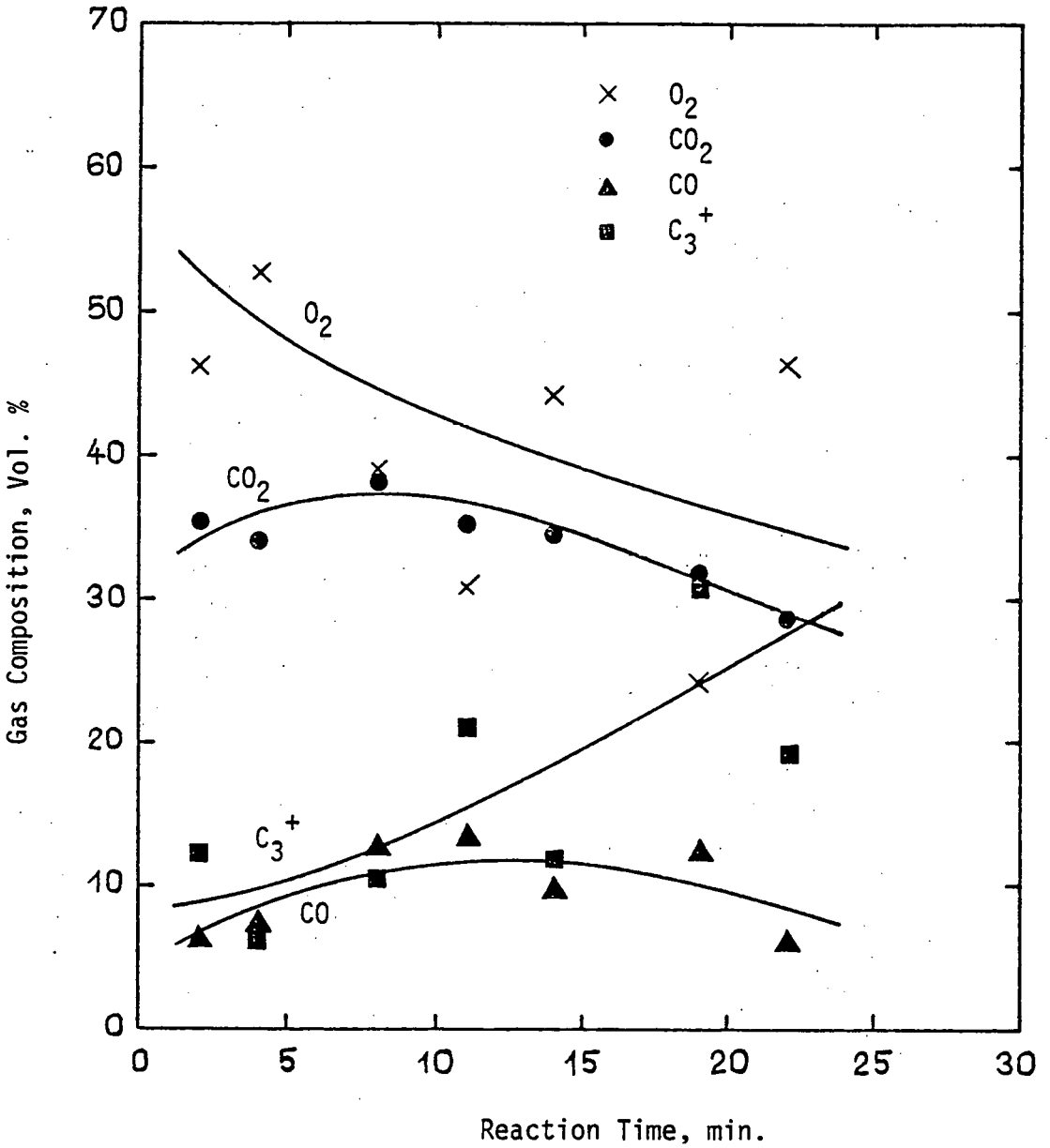

Figure 23: Gas Composition, Reactor Temperature 392°C

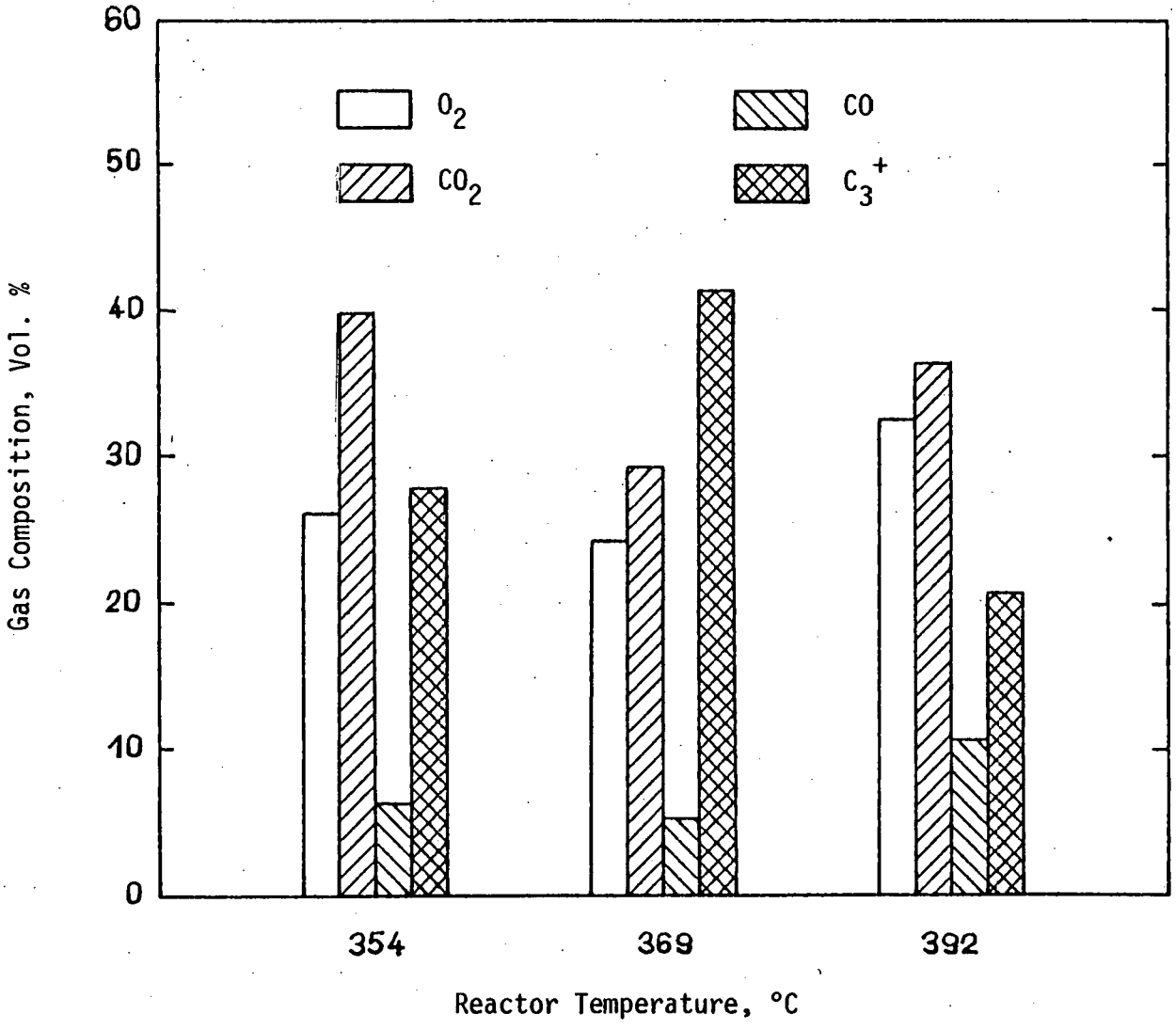

Figure 24: Gas Composition at Different Reactor Temperatures

C_3^+ formation is not available while at higher temperatures they are formed but quickly decomposed to smaller molecules.

4.3.2 Tar

The tar obtained from pyrolysis of cellulosic materials consists of a wide variety of compounds. According to Shafizadeh (4) the major compound in the tar is levoglucosan (~20 percent). In order to get a qualitative estimate about the composition of the tar collected in this investigation two analyses were performed. An elemental analysis was performed on tars collected at four different reactor temperatures. Thin layer chromatography (TLC) and column chromatography were carried out on a mixture of tars collected at different reactor temperatures.

The results of the elemental analysis are shown in Figure 25. The elemental analysis of wood is also indicated for comparison. Figure 25 shows that the oxygen content in the tar is increased with increasing reactor temperature while hydrogen and carbon contents are decreased. This is probably due to the formation of low molecular weight hydrocarbons at higher reactor temperatures.

Attempts were made to separate the tar into the different compounds and identify them. First the tar separability was studied by TLC. The best separation was obtained on silica gel layer irrigated with a 1:1 mixture of chloroform and methyl ethyl ketone. According to the chromatogram shown in Figure 26 the tar consisted of seven compounds.

A mixture of the tars obtained at different reactor temperatures was then dissolved in methyl ethyl ketone and was separated on a silica gel column. The result of the separation is shown in Figure 27. It was

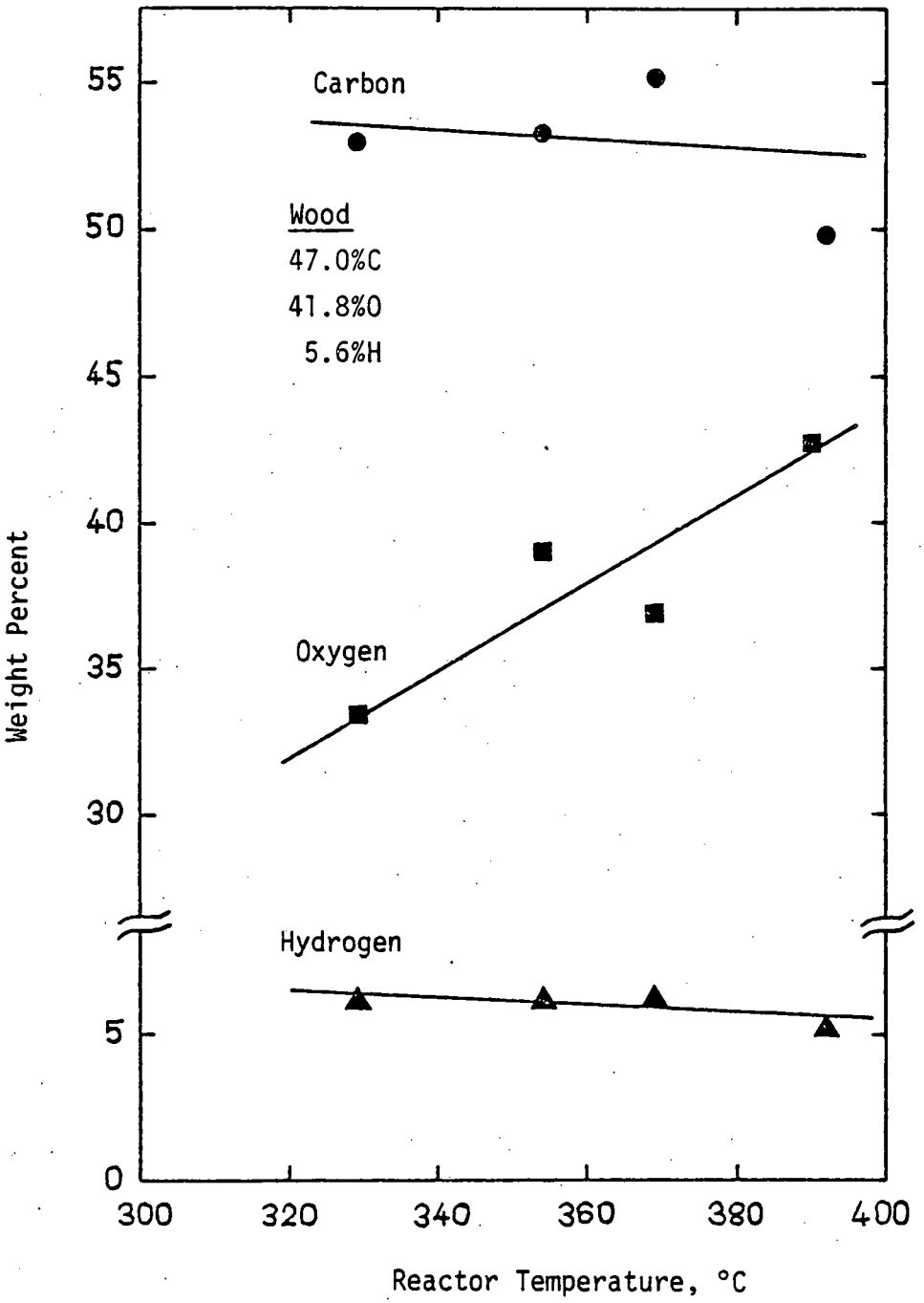

Figure 25: Elemental Analysis of Tar

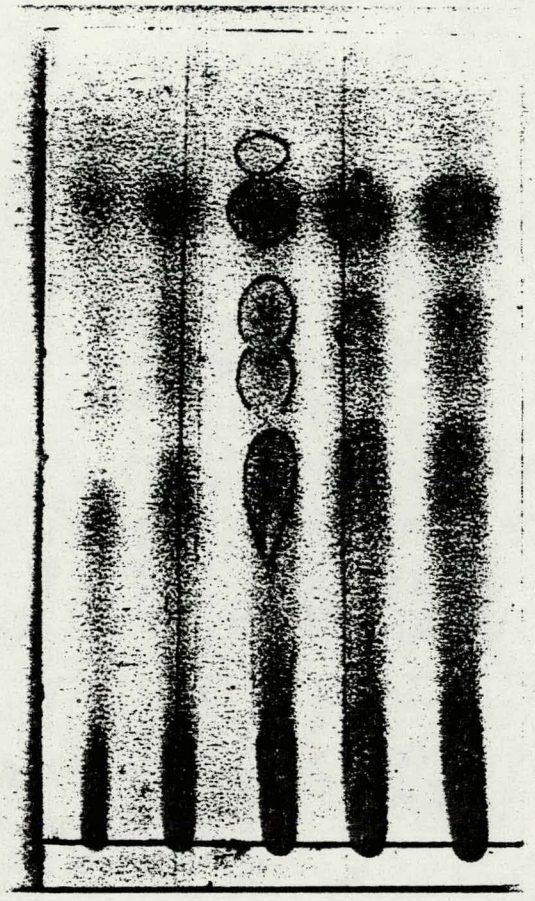

Figure 26: Thin Layer Chromatogram of Tar

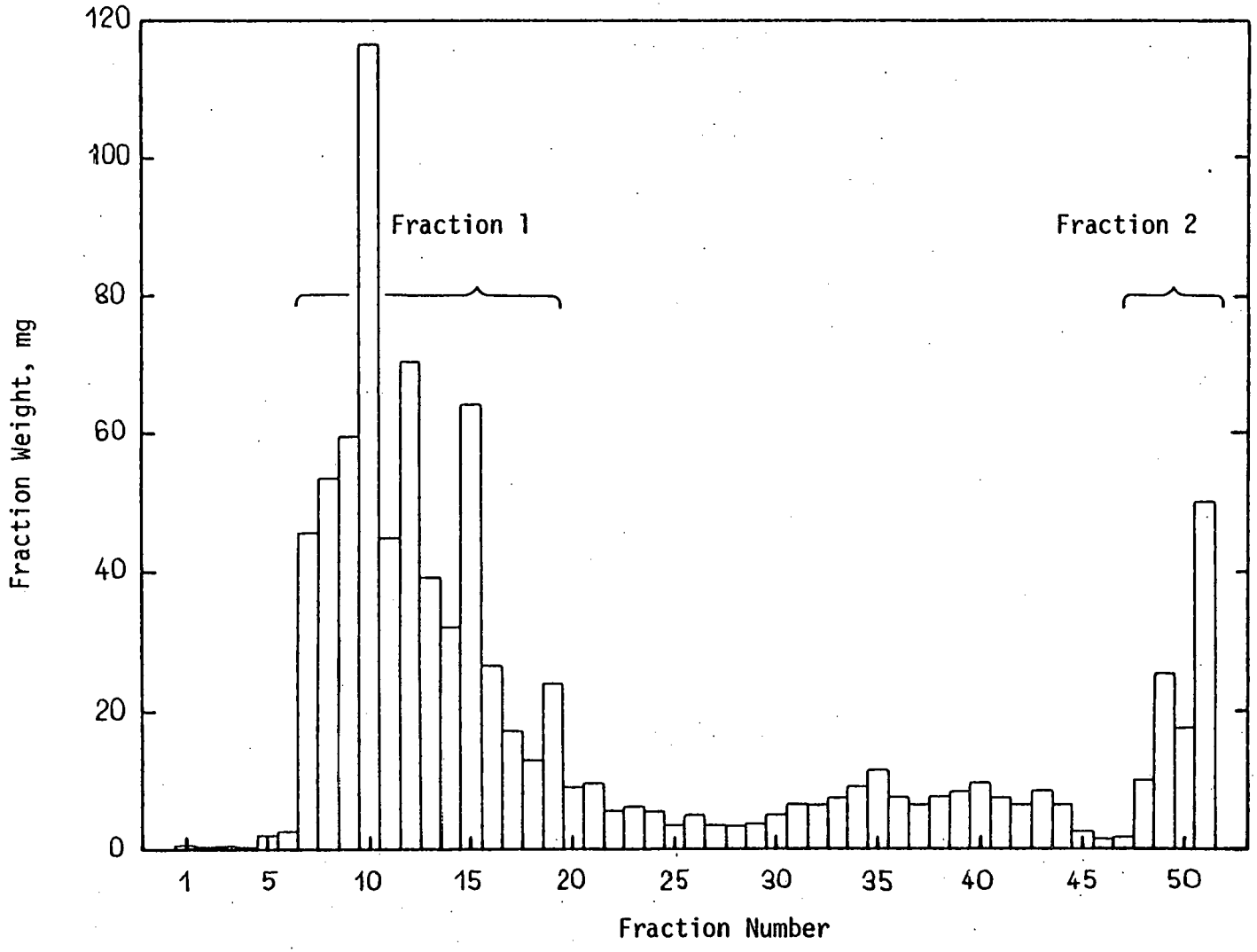

Figure 27: Column Chromatography of Tar

possible to separate the tar into two main fractions. TLC suggested that fraction 1 was a mixture of three compounds and fraction 2 consisted of one compound. The fractions collected between the two main fractions were a mixture of three or four compounds.

An attempt was made to identify the compound in fraction 2 by IR-analysis. The IR-spectrum of fraction 2 corresponded to the spectrum obtained for pure levoglucosan. Another indication that fraction 2 was probably levoglucosan was the fact that like levoglucosan it was insoluble in methyl ethyl ketone.

4.3.3 Char

Very little information is available about the composition of char. In this investigation elemental analysis of chars obtained at four different reactor temperatures were performed. Figure 28 shows the result of the elemental analyses. The elemental analysis is also indicated for comparison. The figure shows that the carbon content is increased with increasing temperature while oxygen and hydrogen contents are decreased. The reason for that is probably the formation of char by dehydration of wood. With increasing temperature the dehydration is increased resulting in less hydrogen and oxygen.

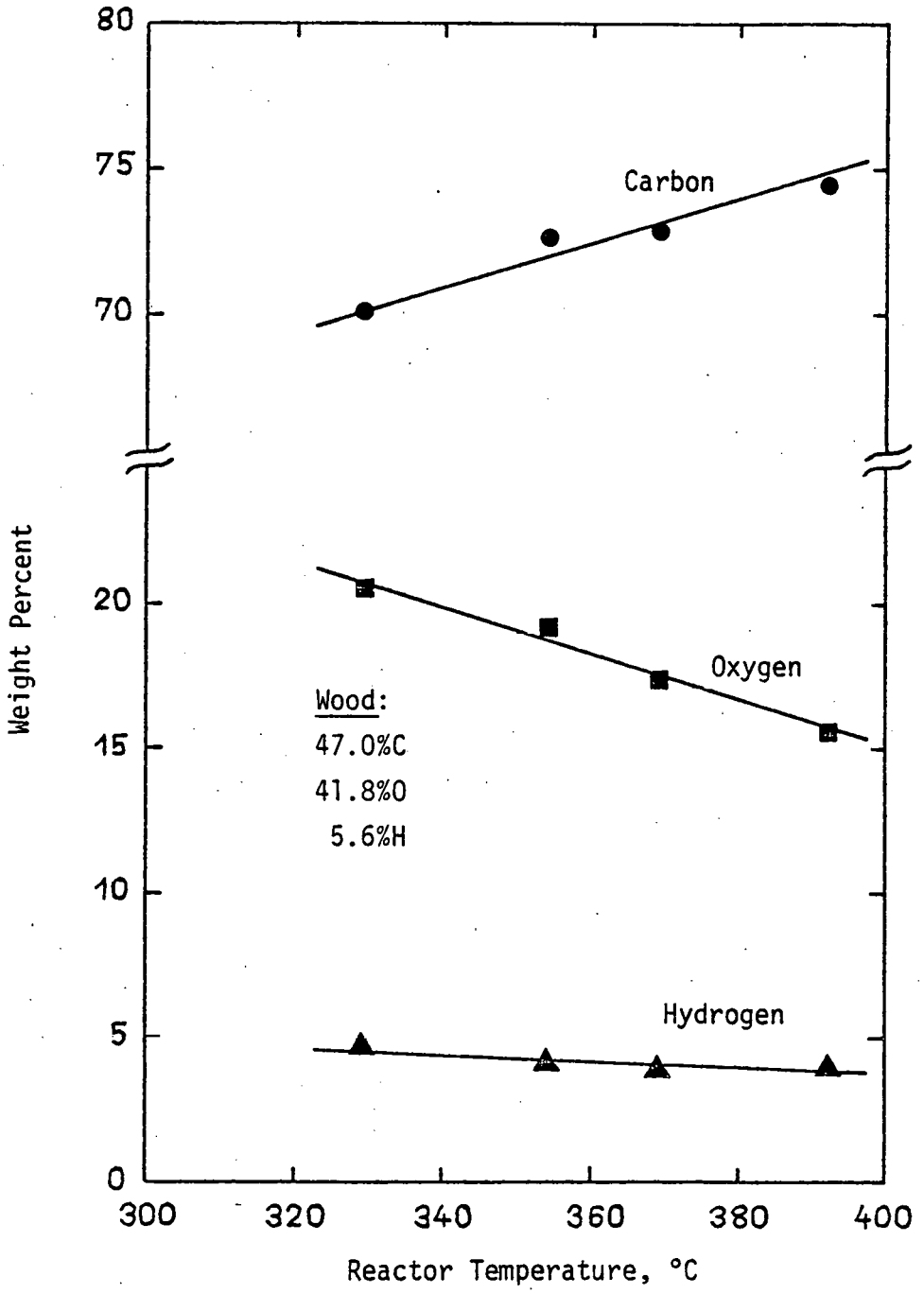

Figure 28: Elemental Analysis of Char

5. CONCLUSIONS

1. For temperatures below 450°C and particles smaller than 2 mm the chemical reaction is the rate-controlling step of the pyrolysis of oak sawdust.

2. Between 300 and 400°C the primary reactions of wood pyrolysis can be described by three first-order parallel reactions. The measured activation energies of wood pyrolysis to gas, tar and char are 88.6, 112.7, and 106.5 kJ/mole, respectively.

3. The yield of the pyrolysis products can be predicted satisfactory by using the integral-mean temperature obtained from the temperature-time curve as reaction temperature.

4. The products obtained from the primary decomposition of wood between 300 and 400°C are gas (~20%), tar (~50%) and char (~30%).

5. The gas consists mainly of carbon dioxide, carbon monoxide, oxygen, and C_3^+ - compounds. The gas composition depends on reaction time as well as reaction temperature.

6. The tar generated in the temperature range investigated is a mixture of about seven different compounds. Its major compound is probably levoglucosan.

7. The carbon content of the tar is increased with increasing temperature.

6. RECOMMENDATIONS

Based on the results of this investigation I recommend to continue this investigation and to study the following items:

1. The kinetics of the decomposition of tar should be investigated.

2. The pyrolysis of wood at higher temperature should be studied. In this case heat and mass transfer should be involved in the investigation.

3. The effects of oxygen and steam on the pyrolysis of wood should be investigated.

4. The pyrolysis of other kinds of biomass such as manure and mesquite can be studied using this reactor.

NOMENCLATURE

A = frequency factor, min^{-1}

E = activation energy, kJ/mol

m = mass, gram

t = reaction time, min.

T = reaction temperature, °C or °K

w = mass fraction

Subscripts:

C = Char

G = Gas

R = Residue

T = Tar

W = Wood

LITERATURE CITED

1. Goldstein, I. S., "Wood as a Source of Chemical Feedstocks", AIChE Symposium Series 177, Volume 74, 111 (1978).

2. Wang, M. J., "Fluidized Bed Pyrolysis of Wood", M.S. thesis, Texas Tech University, Lubbock, Texas, August 1979.

3. Shafizadeh, F., Cochran, T. G., and Sakai, Y., "Application of Pyrolytic Methods for the Saccharification of Cellulose", AIChE Symposium Series 184, Volume 75, 24 (1979).

4. Thomas, R. Y., "Wood Structure and Chemical Composition", ACS Symposium Series 43, 1 (1977).

5. Browne, F. L., U.S. Dept. Agr. Forest Serv. Rep. 2136 (1958).

6. Tang, W. K., U.S. Dept. Agr. Forest Serv. Res. Paper, FPL 71 (1967).

7. Antal, M. J., "Thermochemical Conversion of Biomass: The Scientific Aspects", A Report to the Office of Technology Assessment of the Congress of the United States.

8. Antal, M. J., Edwards, W. E., Friedman, H. C., Rogers, F. E., "A Study of the Steam Gasification of Organic Waste", Final Report, EPA University Grant No. R 8048360 10, (1979).

9. SERI, "A Survey of Biomass Gasification, Volume II - Principles of Gasification", Solar Energy Research Institute, Golden, Colorado, July 1979.

10. Maa, P. S., "Influence of Particle Sizes and Environmental Conditions on High Temperature Pyrolysis of Cellulosic Material", Ph.D. dissertation, West Virginia University, Morgantown, West Virginia, 1971.

11. Maa, P. S., Bailie, R. C., "Experimental Pyrolysis of Cellulosic Material", Paper presented at AIChE 84th National Meeting, Atlanta, Georgia, 1978.

12. Roberts, A. F., "A Review of Kinetics Data for the Pyrolysis of Wood and Related Substances", Combustion and Flame, 18, 261 (1970).

13. Kanury, A. M., "Thermal Decomposition Kinetics of Wood Pyrolysis", Combustion and Flame, 18, 75 (1972).

14. Roberts, A. F., and Glough, G., "Thermal Decomposition of Wood in an Inert Atmosphere", Ninth Symposium (International) on Combustion, Academic Press, New York, 158 (1963).

15. Stamm, A. J., "Thermal Degradation of Wood and Cellulose", Industrial Engineering Chemistry, 48, 413 (1956).

16. Shafizadeh, F., Lai, Y. F., and McIntyre, C. R., "Thermal Degradation of 6-Chlorocellulose and Cellulose - Zinc Chloride Mixture", J. Appl. Polym. Sci., 22, 1183 (1978).

17. Atika, K., Rep. Fire Res. Inst. Japan, 9, 50 (1956).

18. Hileman, F. D., Wojcik, L.H., Futrell, J. H., and Einhorn, I. N., "Comparison of the Thermal Degradation Products of -Cellulose and Douglas Fir under Inert and Oxidative Environments", in Thermal Uses and Properties of Carbohydrates and Lignins, Editor Fred Shafizadeh, p. 49-71, Academic Press, New York, 1976.

19. Fairbridge, C., Ross, R. A., and Sood, S. P., "A Kinetic Study of the Thermal Decomposition of Cellulose Powder in Inert and Oxidizing Atmospheres", J. Appl. Polym. Sci., 22, 497 (1978).

APPENDIX A: EXPERIMENTAL DATA

Table A1: Influence of Film Transport

Reactor Temperature 450°C
Reaction Time 10 min.
Particle Size 0.707...1.41 mm

Run Number	Nitrogen Flow Rate	Sample Size	Residue Weight	Tar Weight	Gas Weight	Overall Mass Balance
——	ml/sec	g	wt. %	wt. %	wt. %	wt. %
8	1.19	0.6022	26.0	51.1	15.1	92.2
9	2.42	0.6285	26.2	49.6	17.1	92.9
10	3.74	0.6125	26.9	49.7	13.4	90.0
11	5.00	0.5641	30.0	48.5	14.9	93.4

Table A2: Effect of Interparticle Transport

Reactor Temperature	445°C
Reaction Time	10 min
Nitrogen Flow Rate	3.5 ml/sec
Particle Size	0.707...1.41 mm

Run Number	Sample Size	Sample Height	Residue Weight	Tar Weight	Gas Weight	Overall Mass Balance
———	g	mm	wt. %	wt. %	wt. %	wt. %
12	0.6090	6.0	25.2	48.3	11.5	85.0
13	0.4665	4.5	25.0	47.2	20.9	93.1
14	0.3066	3.0	24.5	42.7	17.8	85.0
15	0.1586	1.5	24.0	32.1	34.1	90.2

Table A3: Effect of Intraparticle Transport

Reactor Temperature 445°C
Reaction Time 10 min
Nitrogen Flow Rate 3.5 ml/sec

Run Number	Sample Size	Particle Size	Residue Weight	Tar Weight	Gas Weight	Overall Mass Balance
	g	mm	wt. %	wt. %	wt. %	wt. %
16	0.4505	0-0.074	30.3	42.3	19.8	92.4
17	0.6462	0.25-0.707	26.7	52.0	17.1	95.8
18	0.7223	1.41-2.00	28.1	47.6	17.2	92.9
19	0.5674	2.00-2.36	29.1	47.5	21.1	97.7

Table A4: Determination of Composition - Time Curve, Reactor Temperature 329°C

Nitrogen Flow Rate 3.44 ml/sec
Particle Size 0.707...1.41 mm

Run Number	Reaction Time	Sample Size	Residue Weight	Tar Weight	Gas Weight	Overall Mass Balance
———	min	g	wt. %	wt. %	wt. %	wt. %
36	4	0.7099	83.9	5.9	8.9	98.7
32	8	0.7229	74.9	12.5	10.1	97.5
37	8	0.7608	71.1	16.1	11.7	98.9
33	15	0.7792	67.5	16.2	11.6	95.3
38	20	0.6520	58.2	21.6	17.5	97.3
34	24	0.6513	63.0	15.1	19.9	98.0
39	30	0.5467	53.2	18.6	24.4	96.2
35	35	0.5783	59.2	15.0	22.8	97.0
40	95	0.6930	37.8			
41	120	0.6930	36.1			
42	200	0.6930	34.0			
43	260	0.6930	33.4			

Table A5: Determination of Composition - Time Curve, Reactor Temperature 354°C

Nitrogen Flow Rate 3.48 ml/sec
Particle Size 0.707...1.41 mm

Run Number	Reaction Time	Sample Size	Residue Weight	Tar Weight	Gas Weight	Overall Mass Balance
———	min	g	wt. %	wt. %	wt. %	wt. %
49	4	0.6963	78.7	9.7	8.1	96.5
20	8	0.6889	62.1	23.1	10.0	95.2
21	12	0.7355	50.0	31.0	14.6	95.6
50	16	0.7164	39.0	40.1	14.1	93.2
22	20	0.7116	41.7	34.4	17.7	93.8
51	25	0.6649	35.4	37.5	18.6	91.5
23	30	0.5676	35.6	31.5	24.1	91.2
52	90	0.5064	30.5			
53	120	0.5064	30.5			

Table A6: Determination of Composition - Time Curve, Reactor Temperature 369°C

Nitrogen Flow Rate 3.52 ml/sec
Particle Size 0.707...1.41 mm

Run Number	Reaction Time	Sample Size	Residue Weight	Tar Weight	Gas Weight	Overall Mass Balance
———	min	g	wt. %	wt. %	wt. %	wt. %
54	3	0.7552	74.3	14.3	8.5	97.1
28	6	0.6561	56.2	26.6	9.6	92.4
29	11	0.7451	38.9	41.5	17.7	98.1
55	14	0.7161	33.5	44.3	21.0	98.8
30	18	0.7105	34.8	41.2	18.9	94.9
56	22	0.6799	32.1	41.2	24.7	98.0
31	26	0.5968	33.5	34.6	23.8	91.9
57	80	0.5384	29.4			
58	110	0.5384	29.0			

Table A7: Determination of Composition - Time Curve, Reactor Temperature 392°C

Nitrogen Flow Rate 3.45 ml/sec
Particle Size 0.707...1.41 mm

Run Number	Reaction Time	Sample Size	Residue Weight	Tar Weight	Gas Weight	Overall Mass Balance
———	min	g	wt. %	wt. %	wt. %	wt. %
44	2	0.6285	71.9	14.3	8.1	94.3
24	4	0.6419	55.1	27.8	11.7	94.6
25	8	0.7534	33.8	45.6	14.8	94.2
45	11	0.6737	30.6	45.7	17.7	94.0
26	14	0.6521	30.7	45.0	17.1	92.8
46	19	0.6334	29.8	45.6	20.3	95.7
27	22	0.5556	29.5	42.2	20.8	92.5
47	60	0.5346	27.3			
48	90	0.5346	26.8			

APPENDIX B: GAS COMPOSITIONS

Table B1: Gas Composition, Reactor Temperature 329°C

Run Number	Reaction Time	CO_2	O_2	CO	C_3^+
———	min	vol. %	vol. %	vol. %	vol. %
36	4	16.7	62.7	1.6	19.1
32	8	23.1	49.9	1.0	26.0
37	8	21.5	49.6	4.0	25.0
33	15	26.4	42.4	1.9	29.3
38	20	19.5	40.8	5.7	34.1
34	24	17.3	31.7	—	51.0
39	30	16.6	43.2	4.8	35.4
35	35	16.0	29.3	—	54.7

Table B2: Gas Composition, Reactor Temperature 354°C

Run Number	Reaction Time	CO_2	O_2	CO	C_3^+
———	min	vol. %	vol. %	vol. %	vol. %
49	4	24.0	61.8	3.7	10.4
20	8	39.6	41.8	4.6	14.0
21	12	31.7	41.8	6.2	20.3
50	16	35.7	38.7	14.4	11.3
22	20	30.6	39.6	5.6	24.3
51	25	27.6	44.2	9.5	18.6
23	30	24.5	35.5	3.0	37.1

Table B3: Gas Composition, Reactor Temperature 369°C

Run Number	Reaction Time	CO_2	O_2	CO	C_3^+
——	min	vol. %	vol. %	vol. %	vol. %
54	3	30.6	51.7	2.2	15.5
28	6	41.0	36.7	7.7	14.6
29	11	28.9	37.3	8.2	25.6
55	14	23.1	14.8	5.7	56.3
30	18	27.8	33.7	7.1	31.4
56	22	22.7	26.5	4.2	46.6
31	26	23.3	42.0	3.8	30.9

Table B4: Gas Composition, Reactor Temperature 392°C

Run Number	Reaction Time	CO_2	O_2	CO	C_3^+
———	min	vol. %	vol. %	vol. %	vol. %
44	2	35.4	46.2	6.2	12.2
24	4	34.0	52.8	7.2	6.0
25	8	38.1	39.0	12.5	10.4
45	11	35.1	30.8	13.2	20.9
26	14	34.5	44.2	9.6	11.7
46	19	31.9	24.2	12.4	31.5
27	22	28.5	46.3	6.0	19.2